Part I

MICROQUASARS AND X-RAY NOVAE

Recent results on X-ray novae and microquasars at radio and infrared wavelengths

Josep Martí (`jmarti@ujaen.es`)
Universidad de Jaén
Departamento de Física
Escuela Politécnica Superior
Virgen de la Cabeza 2, E-23071 Jaén, Spain

Abstract. Observations at radio and infrared wavelengths have provided a significant contribution to our knowledge of X-ray novae and microquasar systems. For instance, radio interferometers are routinely the first ones to provide accurate subarcsec positions allowing further detailed studies. Similarly, infrared spectroscopy of highly obscured systems is the best way to unveil the often elusive nature of their companion star. In this talk I will review some recent findings in this field obtained by both the Very Large Array (VLA) and the Very Large Telescope (VLT). The VLA has a long record of X-ray novae and microquasar observations and R.M. Hjellming did a very remarkable contribution to it. On the other hand, the VLT results have been available only from recent times, but they look no less promising for the future.

Keywords: XTE J1748−288, V4641 Sgr, Cyg X-3, 1E 1740.7−2942, GRS 1915+105

1. Introduction

X-ray novae are binary systems that eventually undergo a significant increase in their X-ray flux due to an episodic enhancement of mass transfer between the normal star and its compact companion (see e.g. Tanaka & Shibazaki 1996). Their discovery normally occurs thanks to space-based observatories in the X-ray domain, where a significant fraction of their total luminosity is released. In many cases, optical-infrared and radio counterparts are also identified inside the error circles provided by X-ray telescopes. The term microquasar is reserved for these cases where the flaring radio counterpart is resolved into relativistic jets. It is conceivable that all X-ray novae or transient events would fall into this category if they were observed adequately before the radio ejecta fades away.

On the other hand, the microquasar group also includes X-ray binary stars with continuous X-ray activity and production of radio jets. We can think of them as persistent microquasar systems, in contrast to their transient relatives associated to X-ray novae events. Nevertheless, this distinction may not be so clear in some objects where repeated transient activity has been observed over the years.

In any case, the most relevant property of microquasars in the Galaxy is their astonishing scaled down similarity with extragalactic quasars and active galactic nuclei, both morphological and physical. The reader is referred to Mirabel & Rodríguez (1999) for a general review of the microquasar field. Here, I will concentrate on a few individual sources where recent observational progress has been obtained at radio and infrared wavelengths with both the VLA and the VLT, respectively.

2. New superluminal microquasars in the Galaxy

The analogy quasar-microquasar was strongly reinforced when the first superluminal microquasar, GRS 1915+105, was discovered (Mirabel & Rodríguez 1994). Very soon another microquasar, GRO J1655−40, displayed the same kind of behavior (Tingay et al. 1995; Hjellming & Rupen 1995). Based on preliminary results made public by Hjellming and collaborators, the census of superluminal microquasars appears to have doubled in the latest two years. The new members in the superluminal group are two transient X-ray sources, namely XTE J1748−288 and V4641 Sgr.

2.0. XTE J1748−288

This object is one of the 1998 X-ray transients detected at radio wavelengths. The VLA images by Hjellming et al. (1998) indicated one-sided collimated ejection of relativistic plasma, with proper motions of ≥ 20 mas d^{-1} and a high degree of linear polarization. For a distance of ≥ 8 kpc, based on H I absorption measurements, the ejection velocities inferred are $\geq 0.93c$ and possibly superluminal. The most remarkable fact concerning XTE J1748−288 is the evidence of interaction between the jets and the surrounding medium. This statement is based on the observation of deceleration and brightening at the leading edge of the jet, as illustrated in Fig. 1.

2.0. V4641 Sgr

This star underwent a very fast X-ray transient event reaching up to 12 Crab units in 1999 September. The associated radio counterpart was extensively monitored by different radio observatories, and a detailed account of radio results is given by Hjellming et al. (2000). These authors report evidence for fast expansion of an elongated radio source, with proper motion estimates in the range 0.4-1.1 arcsecond d^{-1}. This is a very impressive value for an object outside the Solar System and

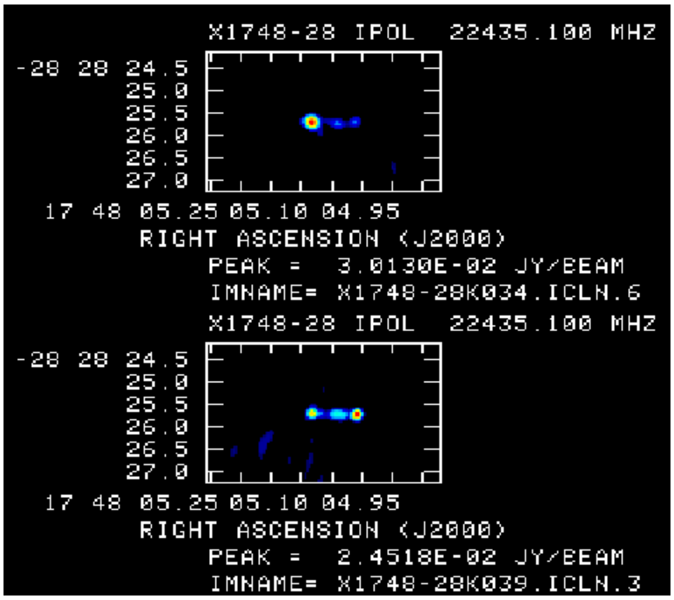

Figure 1. Sequence of VLA images by Hjellming et al. (1998) revealing the ejection and deceleration of a relativistic jet in XTE J1748−288 during 1998 August.

translates into ejection velocities of 1.0-3.2c [d/500 pc]. Although it was not possible to image the detailed movie of the ejection events with the VLA, there is indication of the reliability of the jet structure and the high proper motion. The evidence comes mainly from direct model fitting to the VLA visibilities, together with a good agreement between the multi-frequency light curves and theoretical models for ejection of truncated conical jets.

The distance to V 4641 Sgr is currently a matter of debate. Hjellming et al. (2000) provide some arguments supporting a 500 pc value. However, the recent photometric and spectroscopic analysis by Chaty et al. in this volume strongly indicate a B3-A2 V spectral type and a distance value between 4 and 8 kpc.

2.0. Extended radio jets and double lobe structures

The range of relativistic plasma ejections from microquasars is likely to extend up to very large linear scales, i.e., a fraction of a parsec and possibly beyond. The W50 radio nebula, associated with SS 433, is the only case where such effects are clearly seen up to $\sim$ 50 pc distances (Dubner et al. 1998). Actually, this is not very surprising. Consider for instance the low power jets from young stellar objects, which are able to produce collimated Herbig Haro flows up to several parsec from the

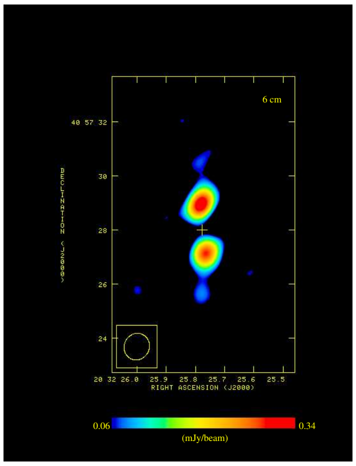

Figure 2. The Cygnus X-3 arcsecond radio jets evidenced after subtracting the variable compact core. The position of the core is indicated by the central cross.

exciting source (e.g. Bally & Devine 1994). In this context, even more dramatic effects should be expected from relativistic jet sources.

Another example could be the case of Cygnus X-3, where only milli-arcsecond radio jets had been reported until not long ago. This microquasar has been recently observed with the VLA by Martí et al. (2000a) in the months following one of its major radio outbursts. After a process of removing the map artifacts introduced by the highly variable compact core, it has been possible to reveal the presence of previously unknown arcsecond radio jets (see Fig. 2). Their inferred linear size and ejection velocities are estimated as ~ 0.2 pc $[d/10$ kpc$]$ and $\sim 0.6c$ $[d/10$ kpc$]$, respectively.

On the other hand, both GRS 1915+105 and Cygnus X-3 have a pair of H II regions that may be extended lobes produced by the relativistic jets (Chaty et al. 2000; Martí et al. 2000a) at huge distances of ~ 100 pc. Unfortunately, the main evidence for a physical connection remains to be the remarkable symmetrical location and position angle coincidence with the jets, thus a chance alignment cannot be strictly ruled out.

3. Microquasars and high energy γ-ray sources

It has been proposed that the luminous star LS 5039 is a new microquasar systems related to one of the unidentified ≥ 100 MeV sources in the 3rd EGRET catalog (Paredes et al. 2000). No other microquasar had been reported before to emit such energetic photons. Further details are given by Paredes et al. in this same volume.

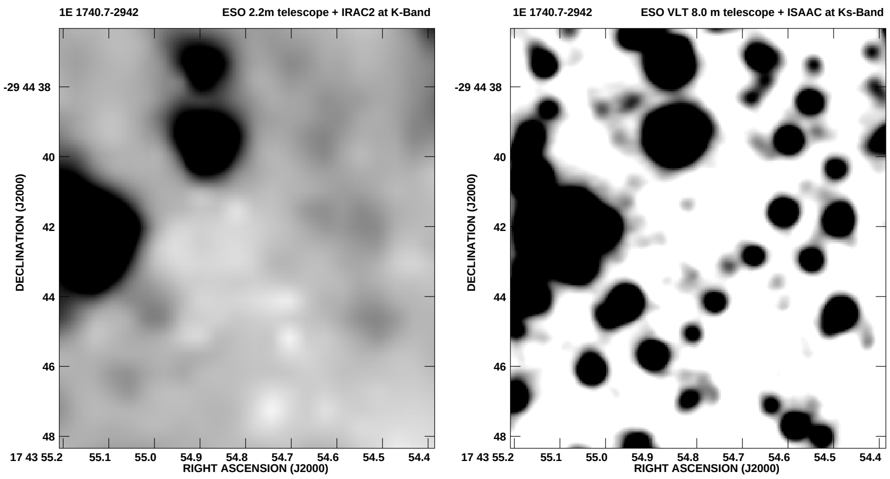

Figure 3. The field of the Galactic Center microquasar 1E 1740.7−2942 as seen in the infrared (K-band) with the ESO 2.2 m telescope (left) and with the VLT (right). The images are centered at the microquasar radio position.

4. Infrared studies of 1E 1740.7−2942 and GRS 1915+105

After many years, there is yet no consensus on the nature of the donor star in these two prototypical microquasars. The new generation of 8 to 10 m telescopes, operating at infrared wavelengths, is possibly the best approach to finally solve the problem. Some interesting results have been already obtained with the 8.2 m unit (Antu) of the VLT and its ISAAC spectro-imager.

4.0. The infrared counterpart of 1E 1740.7−2942

The remarkable improvement in sensitivity obtained by the VLT is clearly evident when comparing the two panels in Fig. 3. In spite of this progress, the VLT has not revealed until now a firm candidate to be the 1E 1740.7−2942 counterpart. The VLT does detect, however, a few sources whose position may be consistent with the radio and X-ray counterpart. These sources are better seen in the expanded view of Fig. 4. All the VLT images in this paper, as well as the information plotted on them, are taken from Martí et al. (2000b) and references therein.

None of the possible candidates, those labelled as 4, 6, 7 and 8 in Fig. 4, has experienced any significant variability that could betray one of them as the counterpart. Under such circumstances, the main obstacle for the identification is the astrometric uncertainty, at the $\sim$

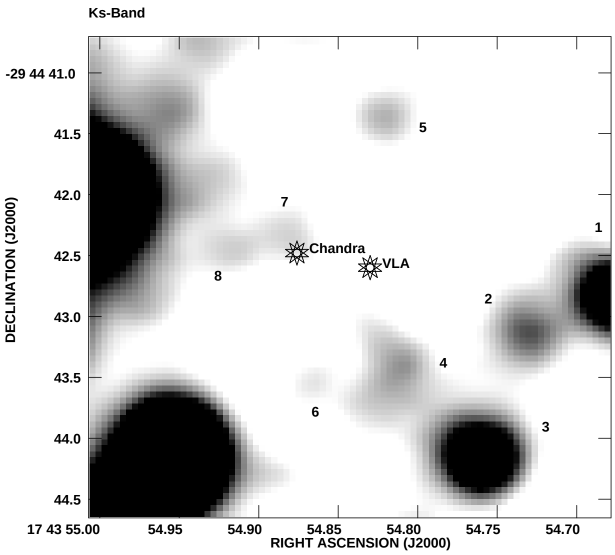

Figure 4. Close up view of the 1E 1740.7−2942 field from the infrared VLT images by Martí et al. (2000b). The VLA radio and Chandra X-ray positions are plotted as star symbols. Only a few sources discussed in the text may be consistent with being the microquasar counterpart.

0.6 arcsecond level, when plotting the accurate VLA radio and Chandra X-ray positions on the infrared frames.

The infrared magnitude of the possible candidate sources is in the range K = 18.5-19.0 mag. These values would agree with a Cygnus X-1 type companion (O9.7 Iab, $M_K = -5.8$) provided that an infrared absorption $A_K \simeq 10$ mag exists. This is equivalent to a hydrogen column density of $N_H \simeq 1.5 \times 10^{23}$ cm^{-2}, i.e., consistent with constrains derived from X-ray spectral fits. Alternatively, if there is no detected counterpart, the $K \geq 19.4$ limiting magnitude (3σ) implies a companion star later than B8 V or earlier than G5 III.

4.0. GRS 1915+105: a high mass X-ray binary?

The infrared counterpart of the first superluminal microquasar has been intensively observed by different authors, but a reliable spectral class is not yet available. The main problems to achieve this goal are mainly: a) the spectral morphology overlap of some star classes in the infrared; b) the difficulties to separate the photospheric and accretion disk contribution; c) the difficulties of correcting for telluric absorptions in the infrared windows. It is also necessary to obtain good spectra, with high signal-to-noise ratio (SNR), in order to facilitate the process

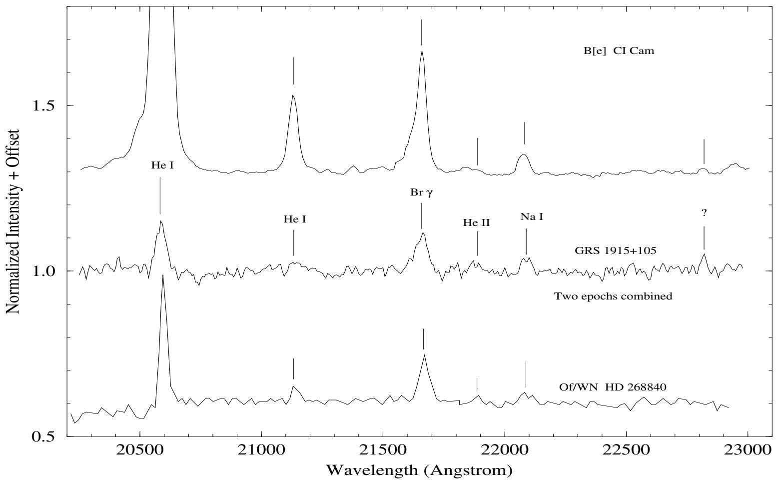

Figure 5. Comparison of the VLT spectrum of GRS 1915+105 in the K-band with those of selected luminous stars (Martí et al. 2000c).

of comparison with spectral standards. Therefore, the large collecting area of the VLT is really of great assistance for this task.

In Fig. 5 the K-band spectrum of GRS 1915+105, as observed with the VLT+ISAAC in low resolution mode, is compared against those of some massive luminous stars. The spectrum in this figure is the result of combining two epochs of observations for better sensitivity (see Martí et al. 2000c for details). At this resolution GRS 1915+105 strongly resembles a high mass star, specially taking into account the new Na I detection. The tentative classification proposed by Martí et al. (2000c) is that of a Of/WN. The possibility of a massive companion is also supported by some spectral features detected in the individual epochs, i.e., a P Cygni profile in quiescence and a blue emission wing in outburst. These features require the existence of an expanding envelope, being blown out during outbursts, and such of circumstellar material is more naturally understood in a high mass system.

Finally, Greiner et al. in this proceedings also report ISAAC observations of GRS 1915+105. Their observed in a higher resolution mode, where high SNR is not always easy to achieve, and conclude that a late type giant companion is the most likely scenario. Further sensitive spectroscopy at all resolutions is therefore required to solve this issue.

Acknowledgements

JM acknowledges partial support by DGICYT (PB97-0903) (Spain).

References

Bally, J. and D. Devine. A parsec-scale "superjet" and quasi-periodic structure in the HH 34 outflow. *ApJ*, 428:L65–L68, 1994.

Chaty, S., et al. A search for possible interactions between ejections from GRS 1915+105 and the surrounding interstellar medium. *A&A*, in press, 2000.

Dubner, G. M., et al. A High-Resolution Radio Study of the W50-SS 433 System and the Surrounding Medium *AJ*, 116:1842–1855, 1998.

Hjellming, R. M. and M. P. Rupen. Episodic ejection of relativistic jets by the X-ray transient GRO J1655−40. *Nature*, 375:464–468, 1995.

Hjellming, R. M., et al. Radio and X-ray Observations of the New Relativistic Jet X-ray Transient XTE J1748−288. *AAS*, 19310308H, 1998.

Hjellming, R. M., et al. Light curves and radio structure for the september 1999 transient event in V4641 Sagittarii (= XTE J1819−254 = SAX J 1819.3−2525). *ApJ*, in press, 2000.

Martí, J., Paredes, J. M. and M. Peracaula. The Cygnus X-3 radio jets at arcsecond scales. *ApJ*, in press, 2000a.

Martí, J., Mirabel, I. F., Chaty, S. and L. F. Rodríguez. VLT search for the infrared counterpart of 1E 1740.7−2942. *A&A*, in press, 2000b.

Martí, J., Mirabel, I. F., Chaty, S. and L. F. Rodríguez. VLT observations of GRS 1915+105. *A&A*, 356:943–948, 2000c.

Mirabel, I. F. and L. F. Rodríguez. A Superluminal Source in the Galaxy. *Nature*, 371:46–48, 1994.

Mirabel, I. F. and L. F. Rodríguez. Sources of Relativistic Jets in the Galaxy. *Annu. Rev. Astron. Astrophys.*, 37:409–443, 1999.

Paredes, J. M., Martí, J., Ribó, M. and M. Massi. Discovery of a high-energy gamma-ray-emitting persistent microquasar. *Science*, 288:2340–2342, 2000.

Tingay, S. J. et al. Relativistic Motion in a Nearby Bright X-Ray Source. *Nature*, 374:141–143, 1995.

Tanaka, Y. and N. Shibazaki. X-ray Novae. *Annu. Rev. Astron. Astrophys.*, 34:607–644, 1996.

Accretion Disk Spectra of Super-luminal Jet Sources and Ultra-luminous Compact X-ray Sources in Nearby Spiral Galaxies

Ken Ebisawa* (ebisawa@subaru.gsfc.nasa.gov)
NASA/GSFC, Code 662, Greenbelt, MD 20771, USA

Aya Kubota, Tsunefumi Mizuno
Department of Physics, The University of Tokyo, 7-3-1 Hongo Bunkyo-ku, Tokyo 113, Japan

Piotr Życki
N. Copernicus Astronomical Center, Bartycka 18, 00-716 Warsaw, Poland

Abstract. The Ultra-luminous Compact X-ray Sources (ULXs) in nearby spiral galaxies and the Galactic super-luminal jet sources share the common spectral characteristic that they have extremely high disk temperatures which cannot be explained in the framework of the standard accretion disk model in the Schwarzschild metric. We have calculated an extreme Kerr disk model to examine if the Kerr disk model can instead explain the observed "too hot" accretion disk spectra. We found that the Kerr disk spectrum becomes significantly harder compared to the Schwarzschild disk only when the disk is highly inclined. For super-luminal jet sources, which are known to be inclined systems, the Kerr disk model may thus work if we choose proper values for the black hole angular momentum. For the ULXs, however, the Kerr disk interpretation will be problematic, as is is highly unlikely that their accretion disks are preferentially inclined.

Keywords: accretion disk, black hole, relativistic jet, X-ray sources

1. The "Too Hot" Accretion Disk Problem

Although X-ray energy spectra of GRS 1915+105 and GRO J1655–40 may be fitted with an optically thick accretion disk plus power-law, which is a canonical model for the high-state black hole candidates, their disk color temperatures can be as high as $\sim$1.3 – 2.0 keV (e.g., Belloni et al. 1997; Zhang et al. 1997; Tomsick et al. 1999); this is significantly higher than other non-jet, well-studied black hole candidates such as Cyg X-1 and LMC X-3, whose disk temperatures are almost always less than $\sim$ 1 keV.

Interestingly, the unusually high disk color temperature, $\sim$1.5–1.8 keV, is also observed from several ultra-luminous compact X-ray sources (ULXs) in IC 342 (Okada et al. 1998), NGC 4565 (Mizuno et al. 1999)

* also Universities Space Research Association

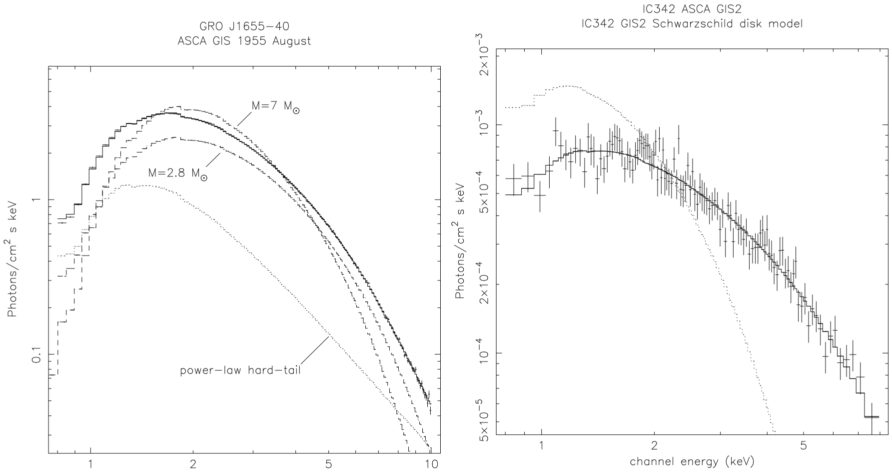

Figure 1. ASCA GIS energy spectra of GRO J1655–40 (left) and the Source 1 in IC 342 (right panel).

and other nearby spiral galaxies; in fact the high accretion disk temperature seems to be a common spectral characteristic of the ULXs (Makishima et al. 2000).

The maximum disk color temperature in the Schwarzschild metric may be written as

$$T_{col}^{(max)} \approx 1.3\,\mathrm{keV}\ \left(\frac{T_{col}/T_{eff}}{1.7}\right)\left(\frac{\dot{M}}{\dot{M}_{Edd}}\right)^{1/4}\left(\frac{M}{7\,M_{\odot}}\right)^{-1/4},$$

where we define the Eddington mass accretion rate as $\dot{M}_{Edd} = 3 \times 10^{18}(M/M_{\odot})$ g s^{-1}, so that $\dot{M}/\dot{M}_{Edd} = 1$ gives the Eddington luminosity. Precise radiative transfer calculation indicates the spectral hardening factor, T_{col}/T_{eff}, is in the range of 1.5 to 1.9, as long as $\sim$ 1 – 10 keV band is concerned (Shimura and Takahara 1995; Ross and Fabian 1996). From this formula, we can see that an optically thick accretion disk around a 7 $M_{\odot}$ Schwarzschild black hole may not be hotter than the color temperature $\sim$ 1.3 keV.

We show examples of the observed "too-hot" accretion disks in GRO J1655–40 (left panel, Figure 1). We applied a Schwarzschild disk model by Hanawa (1989) with the distance and inclination angle being fixed at 3.2 kpc and 70° respectively (Orosz and Bailyn 1997), and $T_{col}/T_{eff} =$ 1.7. The best-fit model disk model was obtained by allowing both mass and mass accretion rate to be free; we have obtained a too small mass $M = 2.8 M_{\odot}$, with $\dot{M} = 2.1 \times 10^{18}$ g s^{-1} ($\dot{M}/\dot{M}_{Edd}$=0.25). If we fix at the most probable mass $M = 7M_{\odot}$ (Orosz and Bailyn 1997), we

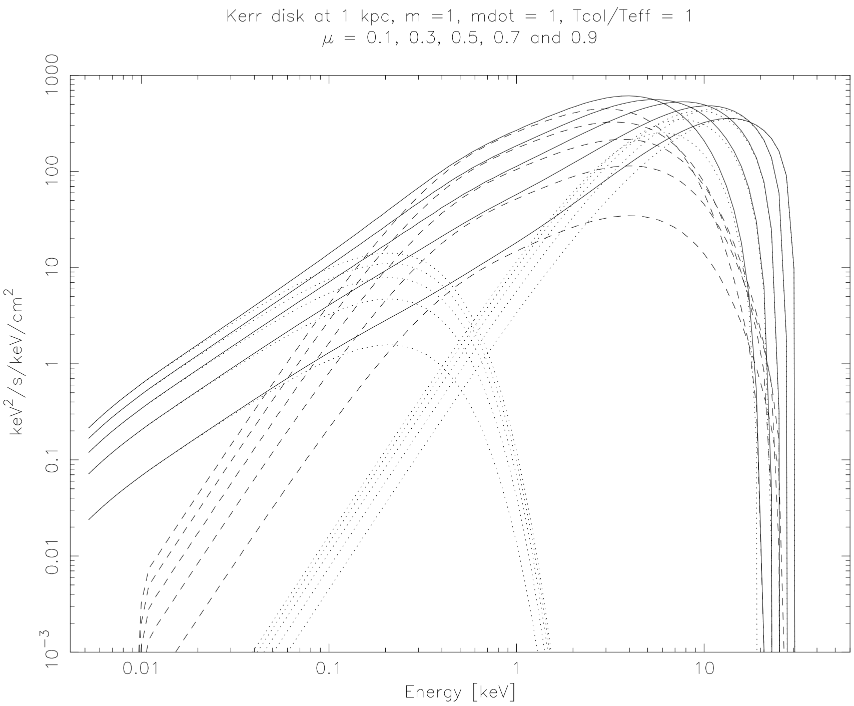

Figure 2. The Kerr accretion disk model with an extreme angular momentum ($a = 0.998$) for the inclination angles $\mu \equiv \cos i = 0.1, 0.3, 0.5, 0.7$ and 0.9. The distance and mass are assumed to be 1 kpc and 1 $M_\odot$ respectively. The Eddington luminosity is assumed, and $T_{col}/T_{eff} = 1$. Solid lines indicate the total disk spectra, and contribution from inner ($1.26\,r_g < r < 7\,r_g$), middle ($7\,r_g < r < 400\,r_g$), and outer parts ($400\,r_g < r$) are also plotted seperately either by dotted or broken lines.

may not achieve the acceptable fit, as the model spectrum is too soft as indicated in the figure.

The right panel in Figure 1 indicates an ASCA spectrum of the “Source 1” in IC342 observed in September 1993 when the source is in the high state (Okada et al. 1998). We fit the observed spectrum with the Schwarzschild disk model by Hanawa (1989), allowing the mass and mass accretion rate to be free parameters, and assuming the face-on geometry. The best-fit model gives $M = 12.6 M_\odot$ and $\dot{M} = 3 \times 10^{20}$ g s^{-1} ($\dot{M}/\dot{M}_{Edd} = 7.9$). Obviously, such a super-Eddington luminosity is very unlikely. For a comparison, we have shown a Schwarzschild disk model spectrum with $M = 100 M_\odot$ at the Eddington limit; it is obvious that the observed spectrum is much harder than the model spectrum.

2. Does Kerr Disk Model Explain the too-hot Disks?

We have calculated the Kerr disk spectrum using the transfer function computed by Laor, Netzer and Piran (1990) for $a = 0.998$. The calculated energy spectra are shown in Figure 2 for several inclination angles.

We have applied the Kerr disk model to GRO J1655–40 and the Source 1 in IC342. For GRO J1655–40, the inclination angle is fixed to $i = 70°$ and $T_{col}/T_{eff} = 1.7$ is assumed. If we allow the mass and mass accretion rate to be free, we obtain $M = 16.4 M_\odot$ and $\dot{M} = 3.5 \times 10^{17}$ g s^{-1} ($\dot{M}/\dot{M}_{Edd} = 0.046$). Compared to the fit with Schwarzschild disk model ($M = 2.8 M_\odot$), significant increase of the mass does indicate the spectral hardening of the Kerr disk model with a large inclination angle. In fact, the derived mass is too large, and further tuning of the angular momentum a will be required to achieve the realistic mass ($7\,M\odot$). Gieliński et al. (2000) calculated the Kerr disk model for several different a values, and found that $a = 0.75$ gives $6.4 M_\odot$ for GRO J1655–40.

IC 342 fit with the face-on Kerr disk model gives (assuming d= 4 Mpc) $M = 27.6 M_\odot$ and $\dot{M} = 2.2 \times 10^{20}$ g s^{-1} ($L = 17\ L_{Edd}$). Only a factor of ~ 2 increase of the mass is due to slight hardening of the face-on Kerr disk model compared to the Schwarzschild one. Note that the super-Eddington problem is not solved. If we assume $i = 80°$, we obtain $M = 340 M_\odot$ and $\dot{M} = 1.7 \times 10^{20}$ g s^{-1} ($L = 1.1\ L_{Edd}$). Then the super-Eddington problem will be almost solved, but such a large mass seems to be unlikely. Also, it is very unlikely that most of the accretion disks in ULXs are inclined when seen from the earth. Therefore, Kerr disk interpretation of the ULXs will be problematic, unless considering some other mechanisms to make the disk spectra apparently harder.

References

Belloni, T. et al. 1997, ApJ, 488, L109
Gieliński, M. et al. 2000, submitted to MNRAS
Hanawa, T. 1989, ApJ, 341, 948
Laor, A., Netzer, H. and Piran, T. 1990, MNRAS, 242, L560
Makishima K. et al. 2000, ApJ 535, 632
Mizuno, T. et al. 1999, PASJ, 51, 663
Okada, K. et al. 1998. PASJ, 50, 25
Orosz, J. A. and Bailyn, C. D. 1997, ApJ, 477, 876
Ross, R. R. and Fabian, A. C. 1996, MNRAS, 281, 637
Shimura, T. and Takahara, F. 1985, ApJ, 445, 780
Tomsick J. et al. 1999, ApJ, 512, 892
Zhang, S. N. et al. 1997, ApJ, 479, 381

BeppoSAX observations of GRS 1915+105

M. Feroci, P. Casella, E. Costa, E. Massaro and P. Soffitta
Istituto di Astrofisica Spaziale, CNR, Roma, Italy

G. Matt
Dipartimento di Fisica, Univ. Roma Tre, Roma, Italy

T. Belloni
Osservatorio Astronomico di Brera, Merate, Italy

A.J. Castro-Tirado
Istituto de Astrofisica de Andalucia, Granada, Spain

V. Dahwan
NRAO, Socorro, New Mexico, USA

F. Frontera
Istituto TESRE, CNR, Bologna, Italy

A. Harmon
Marshall Space Flight Center, NASA, Huntsville, Alabama, USA

F. Mirabel
Service d' Astrophysique, CEA, Saclay, France & IAFE/Conicet, Argentina

G. Pooley
Mullard Radio Astronomy Observatory, Cambridge, UK

M. Tavani
Istituto di Fisica Cosmica, CNR, Milano, Italy

Abstract. The galactic superluminal source GRS 1915+105 was observed by BeppoSAX at several occasions from October 1996 to April 2000. In April 1999 the 2–10 keV light curve showed a long series of quasi regular pulses with a recurrence time of about 50 s. Some preliminary results of a spectral analysis are presented.

Keywords: X-ray sources, accretion disk, microquasar, GRS 1915+105

1. Introduction

The transient source GRS 1915+105 was discovered in 1992 (Castro-Tirado, Brandt & Lund 1992). VLA images of the radio counterpart showed two opposite radio jets moving at an apparent superluminal velocity (Mirabel & Rodriguez 1994) and from their proper motions a distance of about 12 kpc and an inclination angle of about 70° were inferred. The X-ray behaviour of GRS 1915+105 is characterised by alternating bright, very active phases with quiescent periods. Several different modes of variations have been classified by Belloni et al.

(2000). This extreme variability (e.g., Greiner et al. 1996), both in flux and spectrum, has been interpreted by Belloni et al. (1997a) in terms of abrupt emptying of the inner portion of an accretion disk around a black hole, followed by a refilling phase. In this contribution we present the results of a recent observation of GRS 1915+105 performed with three of the Narrow Field Instruments (LECS, MECS and PDS) on board the Italian-Dutch X-ray satellite BeppoSAX.

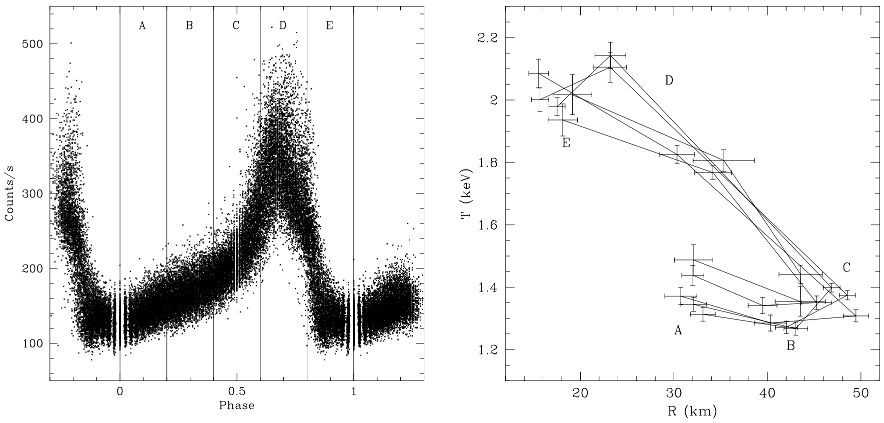

Figure 1. Five phase intervals dividing the folded light curve (left) and the corresponding best-fit spectral parameters for the disk component (right).

2. Observations and Data Analysis

BeppoSAX pointed at GRS 1915+105 several times from October 1996 up to April 2000. In April 1999, during a pointing about 100,000 s long, the source showed a quasi regular train of pulses with a typical recurrence time in the interval from 40 to 60 s. A similar behaviour was observed by Taam et al. (1997) with RXTE and by Paul et al. (1998) with IRS-P3. Individual pulses were evident in the MECS data and not in those of the LECS (< 2 keV) and PDS (> 13 keV), although peaks at the pulse and first harmonic frequencies are prominent in the power spectra. Simultaneous radio observations were carried out at 15 GHz with the Ryle Telescope (UK) and at 8.46 GHz with the VLA: at 15 GHz the source was at the detection limit and at the lower frequency the radio flux was about 1 mJy.

The X-ray spectrum of GRS 1915+105 is complex and strongly variable. Flares are dominated by a soft emission, as apparent from the hardness ratio time series (Belloni et al. 1997a), while a more stable hard component is present. The spectral distribution adopted for these components is a power law extending up to a few hundreds keV superposed to a multitemperature blackbody originating from an accretion disk around a black hole. Spectral fits were carried out using the *diskbb* model included in the *XSPEC* package, based on an equilibrium disk having a radial temperature distribution like $r^{-3/4}$ (Mitsuda et al. 1984). A fixed interstellar column density of 5.5×10^{22} cm^{-2} was also included in the fit.

Once assumed the source distance (12 kpc) and the inclination of the disk to the line of sight (70°) from radio measurements, the only two free parameters of this component are the innermost disk radius R_{in} and the corresponding temperature kT_{in}. These parameters were estimated in five "phase" intervals defined from the folded pulse shapes. Although the pulse duration and shape are both variable, the folded profiles, integrated over a duration of the order of one satellite orbit (100 minutes) remained rather stable and allow to define five intervals of equal length (approximately 10 seconds) starting from the minimum flux time: A, B, C in the rising portion, D centred around the burst maximum, and E during the decay (Fig. 1, left).

The hard component, dominant above 10 keV, can be detected in the PDS data up to about 200 keV. A simple power law fit gives a typical photon index of 3, practically constant over the entire pulse duration. Better fits were obtained using either a power law with an exponential high energy cutoff or a mildly curved spectrum but these improved models did not affect significantly the parameters' values of the thermal component. The estimates of R_{in} and kT_{in} are variable during the pulse. In the first three intervals, when the source luminosity increases slowly, the temperature remains practically constant at about 1.3 - 1.4 keV while R_{in} changes from 32 to 45 - 50 km. During the burst kT_{in} grows to 1.9 - 2.1 keV and, correspondingly, R_{in} becames smaller than 20 km (Fig. 1, right). Comparable values were also found for the 1996 November BeppoSAX observation (Feroci et al. 1999). Paul et al. (1998), despite the similar variability mode, obtained different values: R_{in}, approximately constant during the rising phase, is less than 15 km and rapidly decreasing during the decay, kT_{in} varies between 1 and 2 keV and increases above 3 keV after the maximum.

3. Discussion

The results presented in this contribution, although preliminary, confirm the high complexity of the phenomena observed in GRS 1915+105. Spectral fitting has shown that different at least two components, but possibly more, contribute to its X-ray emission. The generally adopted spectral model is a multitemperature blackbody plus a power law component. Altough the fits are statistically acceptable, the physical meaning of the parameters' best estimates might be questioned. For example, our results imply that in the phase intervals from A to C the R_{in} increases whereas the temperature remains practically constant. According to the equilibrium model (Mitsuda et al. 1984), this finding implies a nearly simultaneous increase of the temperature in the whole disk, or at least the portion emitting the X rays. Furthermore, if taken at face value, a R_{in} value smaller than about 20 km corresponds to a mass for a central Schwarzschild black hole (assuming R_{in}= 6 R_g, i.e. the last stable orbit) less than 2.4 solar masses. This could be due to the crude approximation of the *diskbb* model when the inner disk edge radius and temperature are concerned. A more detailed modelling of the temperature profile at the inner edge of the disk should be used for estimating these parameters.

A crucial question is if the model of a steady, optically thick, multitemperature disk can be applied to our data because the light curve indicates that the source is describing a limit-cycle during a unstable phase. Taam et al. (1997) computed light curves similar to ours in the framework of thermal-viscous instabilities and Szuszkiewicz & Miller (1998) found that during this limit-cycle the disk does not remain optically thick. A future step will be then to perform a spectral analysis by taking into account a time-dependent (non-equilibrium) temperature distribution, changing in the course of the instability cycle.

Acknowledgments: Italian authors are grateful to Italian Space Agency (ASI) for the financial support. NRAO/VLA is a facility of the U.S. National Science Foundation, operated under Cooperative Agreement by Associated Universities Incorporated.

References

Belloni T., Mendez M. et al. 1997a, ApJ 479, L145
Belloni T., Mendez M. et al. 1997b, ApJ 488, L109
Belloni T., Klein-Wolt M. et al. 2000, A&A 355, 271
Castro-Tirado A.J., Brandt S. & Lund N. 1992, IAU Circ N.5590
Feroci M., Matt G. et al. 1999, A&A 351, 985
Greiner J., Morgan E. & Remillard R.A. 1996, ApJ 473, L107
Mirabel I.F. & Rodriguez L.F. 1994, Nature 371, 46
Mitsuda K., Inoue H. et al. 1984 PASJ 36, 741
Paul B., Agrawal P.C. et al. 1998, ApJ 492, L63
Szuszkiewicz E. & Miller J.C. 1998, MNRAS 298, 888
Taam R.E., Chen X. & Swank J.H. 1997, ApJ 485, L83

ASCA observations of the Galactic superluminal sources GRO J1655−40 and GRS 1915+105

Kazutaka Yamaoka*, Yoshihiro Ueda*, Hajime Inoue*, Fumiaki Nagase*, Ken Ebisawa†, Taro Kotani†, Yasuo Tanaka‖

∗ *Institute of Space and Astronautical Science, Yoshinodai 3-1-1, Sagamihara, Kanagawa 229-8501, Japan*

† *NASA Goddard Space Flight Center, Greenbelt, MD 20771, U.S.A.*

‖ *Max-Plank-Institut für extraterresteische Physik, 85740 Garching, Germany*

Abstract. We summarize the *ASCA* observations of the two Galactic superluminal sources GRO J1655−40 and GRS 1915+105, focusing on the absorption line features. The high spectroscopic capability of *ASCA* enabled us to detect iron-K absorption line features from both objects. This is direct evidence for the presence of highly ionized plasma in a non-spherical configuration around a black hole, and is considered to be a unique signature of superluminal jet systems. The candidate of the line-absorber would be a part of an accretion disk at a distance of 10^{9-11} cm from the central X-ray source.

Keywords: GRO J1655−40, GRS 1915+105, X-ray:stars

1. Introduction

The *Advanced Satellite for Cosmology and Astrophysics (ASCA)* (Tanaka, Inoue & Holt 1994) observed the two microquasars GRO J1655−40 and GRS 1915+105 at five and seven occasions, respectively, up to Sept. 2000. Tab. I shows a summary of *ASCA* observations of the two sources. In particular, a continuous multiwavelength campaign over a week was performed in April 2000. The preliminary results are reported by Ueda et al. in this proceeding. The high spectroscopic capability of *ASCA* ($\Delta E/E \sim 2\%$ at 6keV for the SIS (Burke et al. 1994)) enabled us to detect the iron-K absorption line features for the first time from accretion powered X-ray sources. In Tab. I we indicate for each epoch whether the absorption line features were clearly detected or not from the *ASCA* observations. The results of the detailed absorption-line-analyses were reported by Ueda et al. (1998) and Yamaoka et al. (2000) for GRO J1655−40, and Kotani et al. (2000) for GRS 1915+105.

2. Detection of Iron K-absorption Lines

The left panel in Fig. 1 shows the ratio of the SIS data to a continuum model of GRS 1915+105 in the 1994 and 1995 observations when we

Table I. *ASCA* observation summary of GRO J1655−40 and GRS 1915+105

Objects	Epoch	Exposure* [ksec]	Ave. flux†	Iron Kα abs.
GRO J1655−40	1994 Aug.	9	5.6	He-like
	1994 Sep.	19	12	He-like
	1995 Aug.	20	46	H-like
	1996 Mar.	51	0.002	···
	1997 Feb.	57	25	He-like/H-like
GRS 1915+105	1994 Sep.	10	9.8	He-like/H-like
	1995 Apr.	19	21	He-like/H-like
	1996 Oct.	13	24	?‖
	1997 Apr.	16	8.3	?
	1998 Apr.	1	18	?
	1999 Apr.	13	19	?
	2000 Apr.	157	10	?

∗ High bit-rate only.
† In unit of 10^{-9} ergs cm^{-2} s^{-1} in the $2-10$ keV band. The flux of the Crab Nebula corresponds to 2.16×10^{-8} erg cm^{-2} s^{-1} in the same energy band.
‖ Not clearly detected, although weaker Kα absorption lines due to H-like iron ions may be present.

fit the SIS spectra with a Multi-Color Disk (Mitsuda et al. 1986) plus a power law model. As may be seen from this figure, we detected clear absorption line features due to highly ionized iron ions. The central energies of the absorption line features correspond to the Kα line of He-like iron (6.70 keV), and that of H-like iron (6.97 keV).

The right panel in Fig. 1 shows the same plot for GRO J1655−40 in the 1994 August, 1994 September, 1995 and 1997 observations. In addition, we found that the central energy of the absorption lines varied with the continuum X-ray flux from GRO J1655−40. Namely, absorption lines were detected at the energy of the Kα line of He-like iron, of a blend of those of He-like and H-like iron, and that of H-like iron, as the continuum flux increases. This fact strongly suggests that the line-absorber was photoionized by an X-ray irradiation.

In February 1997, we observed GRO J1655−40 with *ASCA* covering one orbital period (2.62 d) of the binary. We divided the whole observation period into four phases and made spectral analysis of each spectrum. Figure 2 shows the equivalent widths of the absorption lines of H-like iron and He-like iron, plotted against the orbital phase. We found no significant changes of the equivalent width associated with the orbital phase, suggesting that the absorber is centered on the black hole and is not affected by the orbital motion of the companion star.

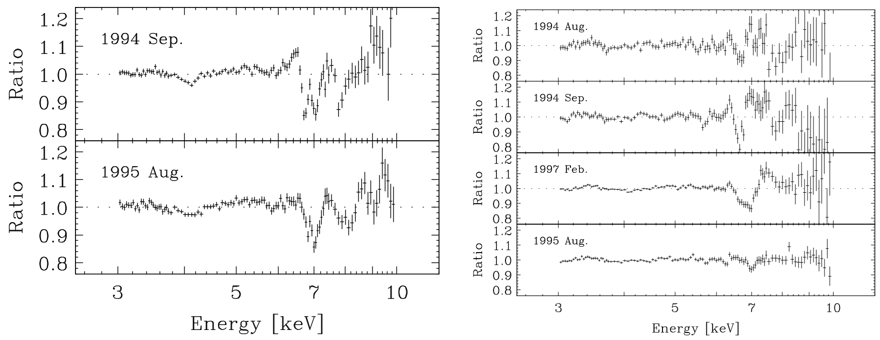

Figure 1. Left panel: SIS spectra of GRS 1915+105 in the 1994 and 1995 observations. Right panel: SIS spectra of GRO J1655−40 in the 1994 Aug.,1994 Sep., 1995 and 1997 observations. The corresponding X-ray intensity increases from upper to lower.

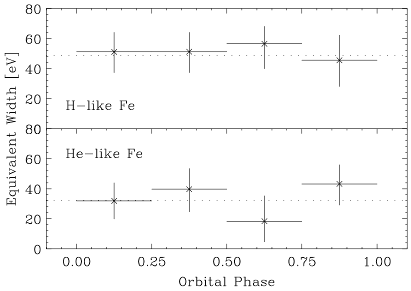

Figure 2. Orbital phase dependence of the equivalent width of H-like and He-like iron Kα absorption lines observed in the 1997 observation of GRO J1655−40.

In case of GRS 1915+105, clear absorption line features due to He-like iron ion were not detected except for the 1994 and 1995 observation, although the presence of a H-like iron absorption lines could be possible. In these epochs, hard X-rays in the $20 - 100$ keV band were high at a level of 0.05 photons cm^{-2} s^{-1}, as detected by the BATSE onboard *CGRO*. This suggests that the hard X-ray emissions might photoionize the plasma to a high ionization stage, which is consistent with the photoionization scenario proposed by Ueda et al (1998).

3. Origin of the Absorption Lines

We can derive two facts from the detection of the absorption lines. One is the presence of highly ionized plasma between an X-ray source and the observer. The other is that the plasma has a non-spherical configuration around a black hole. If the plasma had a spherically symmetric configuration, then the emission lines from outside of our line of sight would fill the absorption lines completely.

Next, we discuss the distance of the line-absorber to the central X-ray source. Let n and r be the number density and the distance of the absorber, the column density nr can be obtained from the curve of growth analysis. Such analyses were already done by Ueda et al. (1998), for GRO J1655−40 and Kotani et al. (2000) for GRS 1915+105, and nr was estimated to be 10^{23-24} cm^{-2}. In addition, so-called ionization parameter ξ ($\equiv L/nr^2$: Tarter, Tucker, & Salpeter 1969) should be around 10^{3-4} ergs cm s^{-1} in order for iron ion to be H-like or He-like according to Kallman & McCray (1982). Using the observed X-ray luminosity L of $\sim 10^{36}$ ergs s^{-1} for GRO J1655−40 and $\sim 10^{37}$ ergs s^{-1} for GRS 1915+105 in difinition of Kallman & McCray (1982), we estimate r to be 10^{9-10} cm and 10^{11} cm, respectively. The higher luminosity of GRS 1915+105 than that of GRO J1655−40 would cause the larger distance of the line-absorber of GRS 1915+105.

The 10^{9-11} cm distance and the constant equivalent width independent of the binary motion would indicate that the line-absorber could be a part of an accretion disk at that distance.

4. Summary

We detect absorption line features due to highly ionized iron from the two Galactic superluminal sources GRO J1655−40 and GRS 1915+105. These may have a connection with superluminal jets and further investigation of the absorption lines will be needed. We summarize the characteristics of the line-absorber as follows. The plasma

- has a non-spherical configuration around a black hole.
- was photoionized by X-ray irradiation.
- has a size of 10^{9-10} cm for GRO J1655−40 and 10^{11} cm for GRS 1915+105.
- shows no orbital phase dependence in GRO J1655−40.

From these observed facts, we conclude that the candidate of the line-absorber would be a part of an accretion disk at a distance of 10^{9-11} cm from the central X-ray source.

References

Burke et al. *IEEE Trans.Nucl.Sci.* 41, 375, 1994.
Kallman, T.R., and McCray, R. *ApJ S* 50, 263, 1982.
Kotani, T. et al. *ApJ* 539, 413, 2000.
Mitsuda, K. et al. *PASJ* 36, 741, 1986.
Tanaka, Y., Inoue, H., and Holt, S.S. *PASJ*, 430, 1994.
Tarter, C.B., Tucker, W., and Salpeter, E.E. *ApJ* 156, 943, 1969.
Ueda, Y. et al. *ApJ* 492, 782, 1998.
Yamaoka, K. et al. submitted to *PASJ*.

Observations of GRS 1915+105 from the USA Experiment on ARGOS

Reba M. Bandyopadhyay
Naval Research Laboratory/NRC, Washington, DC 20375

K.S. Wood, P. Hertz, M.N. Lovellette, P.S. Ray, M.T. Wolff
Naval Research Laboratory, Washington, DC 20375

B. Giebels, E.D. Bloom
Stanford Linear Acclerator Center, Stanford, CA 94309

Abstract. We present first results from a monitoring campaign of GRS 1915+105 undertaken with the USA X-ray timing experiment on the ARGOS satellite. A variety of behaviour has been observed, ranging from low, steady X-ray emission to rapid quasi-periodic flaring on timescales of approximately 10-120 seconds.

1. The USA Experiment

The Unconventional Stellar Aspect (USA) Experiment is one of nine experiments aboard the Advanced Research and Global Observation Satellite (ARGOS) which was launched on 23 February 1999. USA is a collimated proportional counter X-ray telescope with 1000 cm^2 of effective area, sensitive to photons in the energy range 1-15 keV. A unique feature of USA is that all photon events are time tagged by reference to an onboard GPS receiver allowing precise absolute time and location determination.

2. Observations

Here we present first results from a monitoring campaign on the micro-quasar GRS 1915+105 undertaken with USA in 1999 and 2000. We have obtained a total of 255 ks of data, with individual observations ranging in length from 6-23 minutes. One USA count is approximately equal to 0.3 mCrab. A variety behaviour is observed, including steady X-ray emission at several flux levels, rapid irregular $\sim$10 second flaring, quasi-periodic flaring (generally on a timescale of $\sim$60 seconds), and short intervals of "quenching" of the X-ray emission. We have also combined some of our data with simultaneous X-ray data from the RXTE ASM and radio data from the GBI to examine the relationship between the X-ray and radio emission during a radio flaring episode which occurred in November 1999.

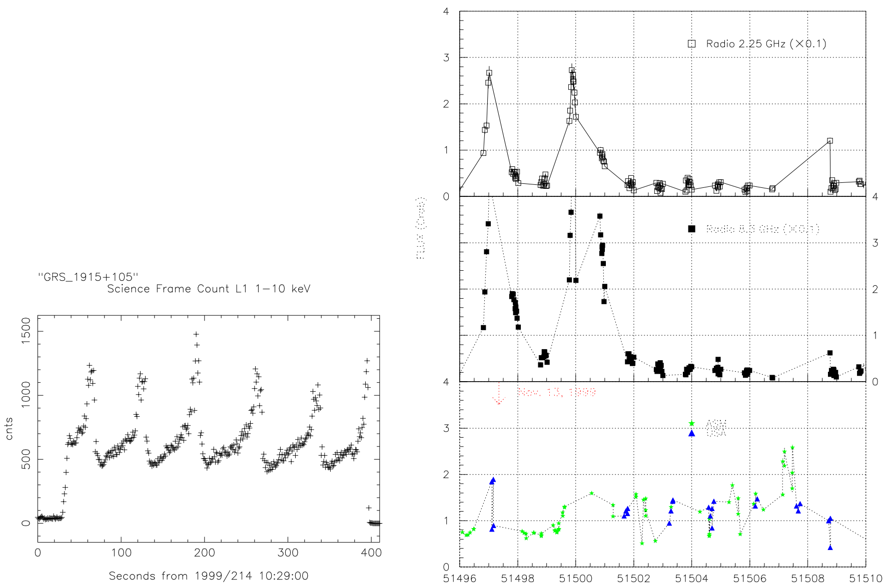

Figure 1. Left: USA X-ray light curve showing quasi-periodic flaring. Right: Radio (GBI, upper panels) and X-ray (combined USA and RXTE ASM, bottom panel) light curves from November 1999. All fluxes have been normalized to 1 Crab.

During July-Aug 1999 and June 2000 USA observed extended intervals of regular quasi-periodic flaring in GRS 1915+105 of the type shown in the left panel of Figure 1. The recurrence time for these flares varies between 30-150 seconds. Bursts of this type have previously been observed by RXTE (Vilhu & Nevalainen 1998) and IAXE (Yadav *et al.* 1999). Our data indicate that in each of these two epochs this bursting behaviour persisted for several *weeks*.

The right panel of Figure 1 shows simultaneous multi-wavelength data from November 1999, with 2.25 and 8.3 GHz radio data from the GBI and X-ray monitoring with USA and the RXTE ASM. The radio flare on MJD 51495 has a clear counterpart in the X-ray light curve, and it appears that the X-ray flare on MJD 51507 is present in the radio emission. Therefore during this two week interval the X-ray and radio flares appear to be correlated, although some previous observations have shown similar radio flares to be anti-correlated with the X-ray emission (*e.g.* Bandyopadhyay *et al.* 1998).

References

Bandyopadhyay R. *et al.* 1998, MNRAS, 295, 623.
Vilhu O. & Nevalainen J. 1998, ApJ, 508, L85.
Yadav J.S. *et al.* 1999, ApJ, 517, 935.

The 2000 April Multiwavelength Campaign of GRS 1915+105

Y. Ueda[1], K. Yamaoka[1], J.E. Grove[2], M. McCollough[3],
P. Durouchoux[4], J. Rodriguez[4], F. Mirabel[4,5], J. Swank[6], M. Feroci[7],
P. Casella[7], A.J. Castro-Tirado[8,9], C. Sanchez-Fernandez[9],
S. Chaty[10], H. Castaneda[11], K. Kohno[12], V. Dhawan[13],
S.A. Trushkin[14], K. Ebisawa[6], T. Kotani[6], H. Inoue[1],
and the multiwavelength campaign team

[1] *Institute of Space and Astronautical Science, Japan*
[2] *Naval Research Lab, USA*
[3] *MSFC/NASA, USA*
[4] *Service d'Astrophysique, Saclay, France*
[5] *IAFE/CONICET, Argentina*
[6] *GSFC/NASA, USA*
[7] *Istituto di Astrofisica Spaziale, C.N.R., Italy*
[8] *IAA-CSIC, Granada, Spain*
[9] *LAEFF-INTA, Madrid, Spain*
[10] *Department of Physics and Astronomy, The Open University, UK*
[11] *Observatorio Astronomico Nacional de Mexico, Mexico*
[12] *Nobeyama Radio Observatory, NAO, Japan*
[13] *NRAO, USA*
[14] *SAO, Russia*

Abstract. We report results from multiwavelength observations of the microquasar GRS 1915+105 performed during the 2000 April campaign. This is one of the biggest campaigns ever made for this source covering the broad band from radio to Gamma-rays. Multiwavelength light curves compiled from all the data reduced up to date and broad band spectra obtained with ASCA and RXTE are presented.

Keywords: GRS 1915+105, multiwavelength observations

1. Observations

The ASCA satellite observed GRS 1915+105 in the 0.5–10 keV band from 2000 April 17 12:00 to April 25 12:00 for a net exposure of 271 ksec. Coordinated with the ASCA observations, simultaneous observations were made with RXTE on April 17, 22 and 23, with BeppoSAX from April 21 to 24 (PI: Feroci), and with OSSE/CGRO from April 18 to 25. From ground, VLA observations were made (PI: Mirabel) on April 17, 22, and 23, IR (K band) photometric monitoring at Calar Alto from April 18 to 25 (PI: Castro-Tirado), at the ESO from April 17 to 23 (PI: Chaty) , and at Mexico (PI: Castaneda) from April 22 to 25, and radio observations (at 3.2 mm) at the Nobeyama Millimeter Array from April 17 to 19 (PI: Kohno). In addition, monitoring data of the GBI(2.25 GHz and 8.3 GHz), ASM/RXTE (1.5-12 keV), and BATSE/CGRO (20-100 keV) are available. Results of timing analysis using the RXTE data are reported by Rodriguez *et al.* (2000). More detailed analysis of the IR K' data is reported in Sánchez-Fernández (2001).

2. Results

Multiwavelength light curves obtained from this campaign are shown in Figure 1. We list several results noticed from the light curves.

- The soft X-rays showed rapid oscillations in the first half of the campaign (see below). Daily averaged 2–10 keV fluxes are $(0.9 - 1.1) \times 10^{-8}$ erg s^{-1} cm^{-2}.
- The hard X-ray flux (20–100 keV) and the radio fluxes (2.25 GHz and 8.3 GHz) were around the levels of the "plateau" state defined by Foster *et al.* (1996).
- The OSSE flux (50–300 keV) showed a significant variability on hours to days. The photon index is about 3.
- The IR K-band fluxes in these data were mostly at a quiescence level (e.g., Fender *et al.* 1997) and seemed to correlate with the soft X-ray intensity on timescale of hours. A weak flare was detected at MJD = 51654.08.

Before MJD$\simeq$51655, the source showed a peculiar pattern of variability (class ν in Belloni *et al.* 2000), characterized by a rapid oscillation lasting for typically 500–1000 sec, followed by a decline of $\sim$ 200 sec and a slow rise of $\sim$ 1000 sec. The soft X-ray intensity and the hardness have correlations: when the intensity is high, the spectrum becomes hard in the 0.7–10 keV range but soft in the 3–31 keV range. We here define three characteristic states: (1) the "oscillation high" state, when the soft X-ray flux is high during the oscillation (>1800 c s^{-1} per PCU in the 16 sec resolution light curve) , (2) the "oscillation low" state (<1800 c s^{-1} per PCU), and (3) the "rise" state, when the intensity increases linearly with time between oscillations.

We make a joint spectral analysis of the ASCA/GIS, RXTE/PCA, and RXTE/HEXTE data, covering the 1–150 keV band. The spectra are created separately for the 3 states defined above, although the ASCA and RXTE data are not exactly simultaneous. Figure 2 shows unfolded spectra for each state. The normalization of the oscillation-high and - low state spectra is multiplied by 9 and 3, respectively, for

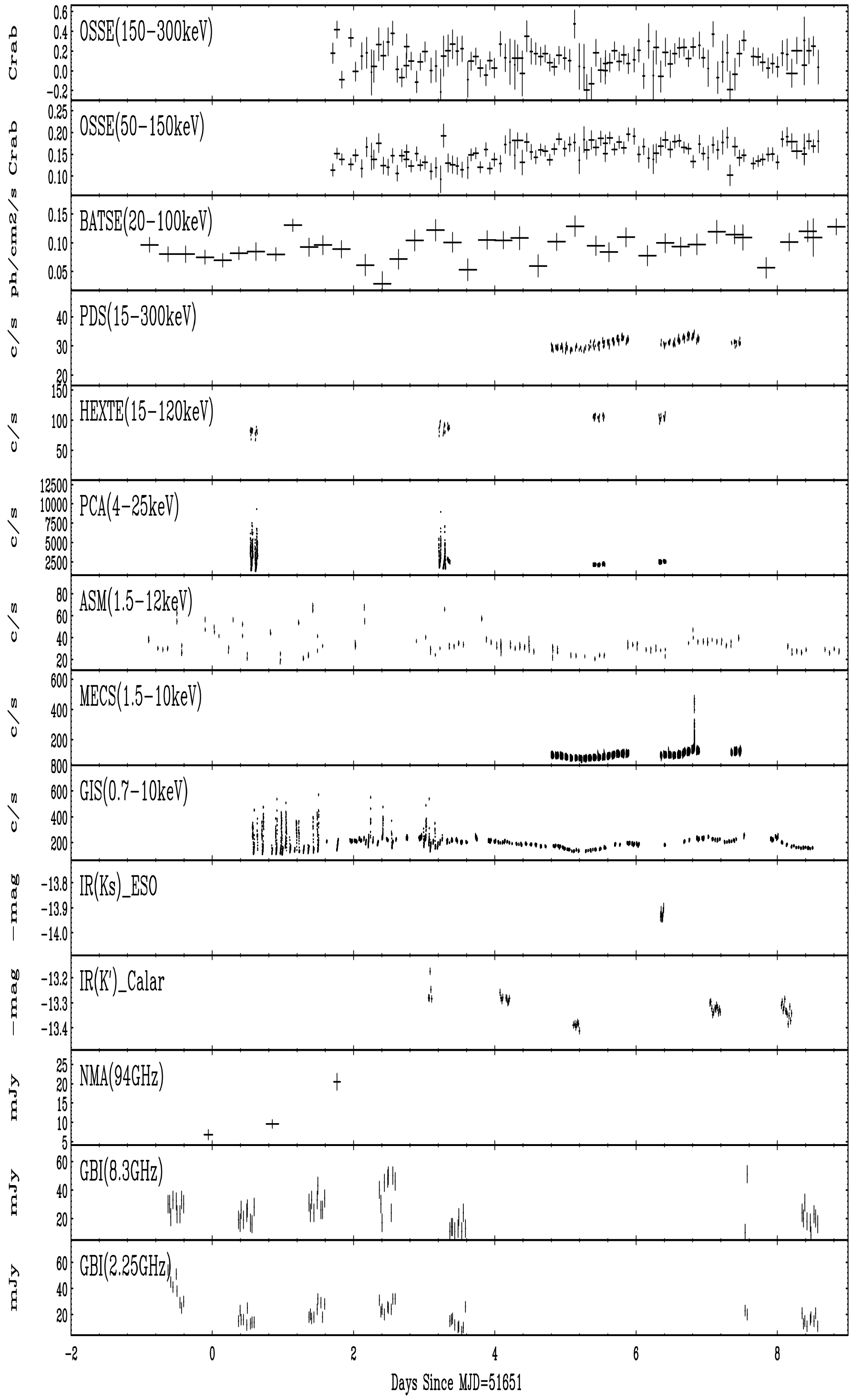

Figure 1. Multiwavelength light curves of GRS 1915+105 during the 2000 April campaign, covering between April 16 and 25. They are sorted in energy band (higher energy in upper). The reference day (MJD 51651) corresponds to 2000 April 17.0 (UT).

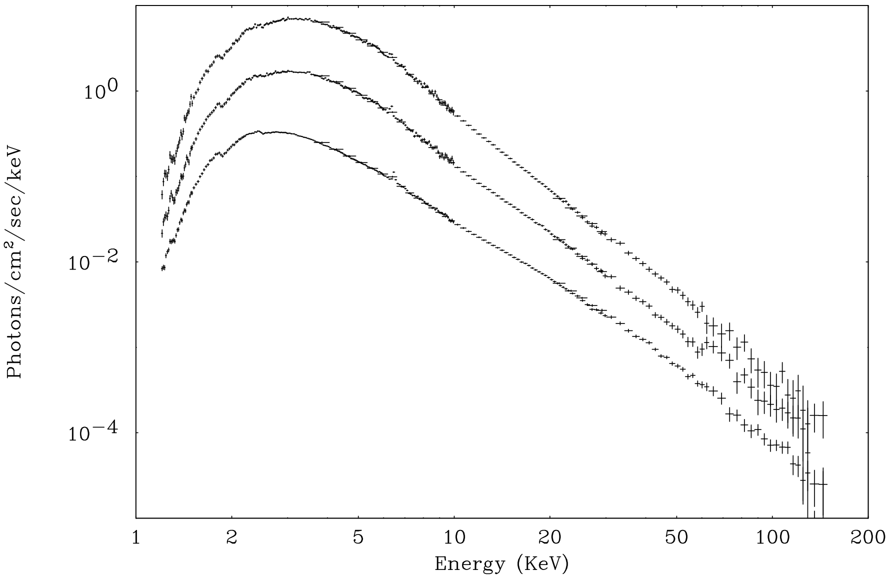

Figure 2. The unfolded spectra of GRS 1915+105 in different states, obtained by joint analysis of the GIS, PCA, and HEXTE spectra. Upper: oscillation high (normalization $\times 9$), middle: oscillation low ($\times 3$), and bottom: rise ($\times 1$). The continuum is modeled by the multicolor disk model plus a Comptonized blackbody.

plotting purpose. Preliminary analysis indicates that the contribution of a disk component is much weaker in the rise state than in the oscillation state although the difference of the hard band spectrum above 20 keV is not conspicuous between these states. Detailed spectral analysis and the implications of the results will be presented in future papers.

Acknowledgements

This research has made use of the data of the Green Bank Interferometer (GBI), which is a facility of the National Science Foundation operated by the NRAO in support of NASA High Energy Astrophysics programs.

References

Belloni, T. *et al.* 2000, A&A, in press (astro-ph/0001103)
Fender, R.P. *et al.* 1997, MNRAS 290, L65
Foster, R.S. *et al.* 1996, ApJ 467, L81
Mirabel, I.F. *et al.* 1998, A&A 330, L9
Rodriguez, J. *et al.* 2000, in preparation
Sánchez-Fernández, C. 2001, Ph.D. Thesis, Madrid

Identification of the donor in GRS 1915+105

J. Greiner and M.J. McCaughrean
Astrophysical Institute Potsdam, 14482 Potsdam, Germany

J.G. Cuby
ESO, Alonso de Córdova 3107, Santiago 19, Chile

A.J. Castro-Tirado
Instituto de Astrofísica de Andalucía, E-18080 Granada, Spain
Laboratorio de Astrofísica Espacial y Física Fundamental, E-28080 Madrid, Spain

R.E. Mennickent
Universidad de Concepción, Casilla 160-C Concepcion, Chile

Abstract. We report on medium-resolution H and K band spectroscopy of GRS 1915+105 using the 8m VLT at ESO. We clearly identify absorption bandheads from ^{12}CO/^{13}CO. Together with other features we classify the donor as a K-M III star.

Keywords: X-ray binary, GRS 1915+105, infrared observations

1. Introduction

GRS 1915+105 (Castro-Tirado et al. 1992, 1994) is the prototypical microquasar, a galactic X-ray binary ejecting plasma clouds at v≈0.92 c (Mirabel & Rodriguez 1994). It exhibits unique X-ray variability patterns (Greiner et al. 1996) which have been interpreted as instabilities leading to an infall of parts of the inner accretion disk (Belloni et al. 1997). It is therefore of great importance to know some details about the system components in order to understand the conditions which lead to these unique characteristics.

2. Observations and Results

We obtained H and K band infrared spectroscopy of GRS 1915+105 with the aim of searching for absorption signatures due to the donor. Since GRS 1915+105 is a strongly variable infrared source, believed to predominantly caused by synchrotron emission of ejected material (Eikenberry et al. 2000, Greiner et al. 2001), this required high signal-to-noise as well as good spectral resolution in order to beat the strong veiling. We therefore used the infrared spectrometer ISAAC on the 8m VLT Antu telescope on Paranal (ESO, Chile).

The short wavelength (0.9–2.5 μm) arm of ISAAC is equipped with a 1024×1024 pixel Rockwell HgCdTe array with an image scale of

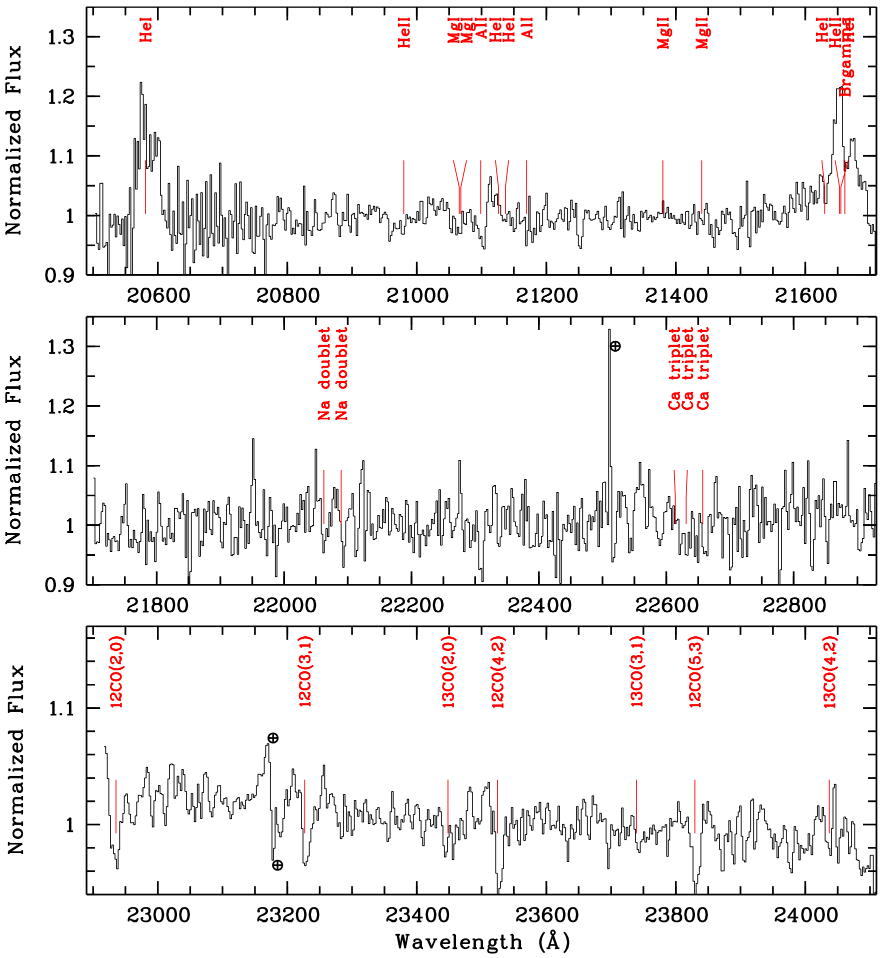

Figure 1. Spectrum of GRS 1915+105 in the K band. The top two panels correspond to 3000 sec exposure, while the bottom panel shows a sum of 4 images with 2000 sec exposure each. All spectra were rebinned by a factor of 2.

$0\farcs147$/pixel. Using the grating with the highest possible spectral resolution (∼3000 for a 1″ slit) yields 0.8Å/pixel in the H band and 1.2Å/pixel in the K band. Observations were performed in 1 (2) adjacent H bands, and 2 (3) adjacent K bands on 20/21 July 1999 (24/25 July 2000).

Science exposures consisted of several 250–300 sec individual exposures which were dithered along the slit by ±30″. In order to correct for atmospheric absorption, the nearby star HD 179913 (A0 V) was observed either before or after each science exposure. The initial data reduction steps like debiasing, flatfielding and co-adding were performed within the *Eclipse* package (Devillard 2000). The extraction and wavelength calibration was done using an optimal extraction routine within the MIDAS package.

The spectra of the 3 grating settings covering the K band are shown in Fig. 1. The top panel shows the strong emission lines of Br γ and He I known already from previous low-resolution spectroscopy (Castro-Tirado et al. 1996). In addition, we find for the first time several absorption lines which allow us to roughly identify the donor in GRS 1915+105. The lower panel clearly shows ^{12}CO absorption band heads characteristic of a low temperature ($T < 7000$ K) star (e.g. Kleinmann & Hall 1986). Though weak, we also identify the ^{13}CO (2,0) and ^{13}CO (3,1) transitions, indicating a luminosity class III or brighter (e.g. Wallace & Hinkle 1997). We also identify the Na doublet (2.20624/2.20897 μm), and possibly the Ca triplet (2.26141/2.26311/2.26573 μm), Al I (2.10988 μm) and the Mg I doublet (2.10655/2.10680 μm) in absorption. Note that the CN doublet (2.0910/2.0960 μm), which in supergiants is more prominent than Al/Mg, is not detected. Thus, we conclude that the donor in GRS 1915+105 is a late-type K-M giant.

We have tried to confirm the luminosity class more quantitatively by using the veiling-independent indicator

$r = \log[EW(^{12}\mathrm{CO}(2,0))/(EW(\mathrm{Na}) + EW(\mathrm{Ca}))]$

(Ramírez et al. 1997). Because of the low significance of the Ca triplet our measurement has a large error: $r = 0.25 \pm 0.20$. This value falls in between the ranges covered by dwarfs ($-0.2 \lesssim r \lesssim 0.0$) and giants ($0.4 \lesssim r \lesssim 0.6$) (Ramírez et al. 1997). The ratio of equivalent widths of ^{12}CO to ^{13}CO which depends on luminosity class (Campbell et al. 1990), has been measured for the seven transitions covered (lower panel of Fig. 1) to $\sim 3 \pm 1$, again supporting a giant classification.

Unfortunately, the H band spectra are of too low S/N ratio to detect OH or CO, thus not allowing us to use the veiling-independent temperature/luminosity discriminants as proposed by Meyer et al. (1998). However, the veiling was roughly determined by comparison of our flux-calibrated 2.35 μm spectrum of GRS 1915+105 with that of a K2 III standard star, observed with the same settings. We adopted a 13 mag flat continuum and added the K2 III star spectrum scaled to a brightness in the range 13.5–17.5 mag (Fig. 2). A comparison with the GRS 1915+105 spectrum gives a (not extinction-corrected) magnitude of K = 14.5–15.0 mag for the donor. With a distance of ~11 kpc and a $A_{\mathrm{K}} = 3$ mag extinction correction this implies an absolute magnitude of $M_{\mathrm{K}} = -2...-3$ mag, consistent with the giant classification.

This identification of the donor of GRS 1915+105 as a K-M giant implies a rather narrow mass range of 1.0–1.5 $M_{\odot}$. Typical spherical mass-loss rates of such stars are much too low to sustain the high accretion luminosity of GRS 1915+105 via accretion from the donor's stellar wind. We therefore suggest (not too surprisingly) that accretion should occur via Roche lobe overflow. We finally note that while our

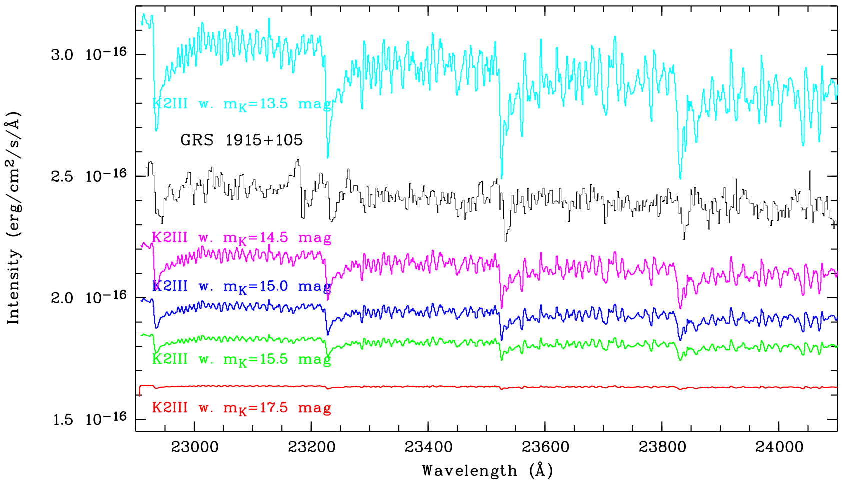

Figure 2. Spectrum of GRS 1915+105 in the 2.3–2.4 μm range (second from top, not extinction-corrected), compared to the spectrum of the K2III star HD 202135 scaled to different magnitudes (as marked on each spectrum) which is veiled by a 13 mag flat continuum. This implies that the donor of GRS 1915+105 has a magnitude of 14.5–15 mag prior to extinction correction.

identification contradicts the findings of Martí et al. (2000) who argue for a massive OB-type companion, it is consistent with the constraints derived by Eikenberry et al. (2001).

The presence of clear donor absorption features will now allow a period search as well as a determination of the mass of the compact object using radial velocity measurements of the donor.

References

Belloni T., Mendez M., King A.R., et al. 1997, *ApJ* 479, L145
Campbell B., Lambert D.L., Maillard J.-P., 1990, *PASP* 102, 79
Castro-Tirado A.J., Brandt S., Lund N., 1992, IAU Circ. 5590
Castro-Tirado A.J., Brandt S., Lund N., et al.1994, ApJS 92, 469
Castro-Tirado A.J., Geballe T.R., Lund N., 1996, ApJ 461, L99
Devillard N., 2000, Eclipse Users Guide, www.eso.org/projects/aot/eclipse/eug/index.html
Eikenberry S.S., Matthews K., Muno M., et al. 2000, *ApJ* (astro-ph/0001472)
Eikenberry S.S., et al. 2001, these proc.
Greiner J., Morgan E.H., Remillard R.A., 1996, *ApJ 473*, L107
Greiner J., Vrba F.J., Henden A.A., Guetter H.H., Luginbuhl C.B., 2001, these proc.
Kleinmann S.G., Hall D.N.B., 1986, *ApJ Suppl.* 62, 501
Martí J., Mirabel I.F., Chaty S., Rodriguez L.F., 2000, *A&A* 356, 943
Meyer M.R., Edwards S., Hinkle K.H., Strom S., 1998, *ApJ* 508, 397
Mirabel I.F., Rodriguez L.F.: 1994, *Nature* 371, 46
Ramírez S.., Depoy D.L., Frogel J.A., Sellgren K., Blum R.D., *AJ 113*, 1411
Wallace L., Hinkle K., 1997, *ApJ Suppl.* 111, 445

UKIRT IR spectra of the microquasar GRS 1915+105

Emilios Harlaftis
Institute of Astronomy and Astrophysics, National Observatory of Athens, P. O. Box 20048, Athens 118 10, Greece

Vik S. Dhillon
Department of Physics and Astronomy, Univ. of Sheffield, Sheffield S3 7RH, UK

Alberto J. Castro-Tirado
Instituto de Astrofísica de Andalucía (IAA-CSIC), P.O. Box 03004, E-18080 Granada, Spain; and Laboratorio de Astrofísica Espacial y Física Fundamental (LAEFF-INTA), P.O. Box 50727, E-28080 Madrid, Spain

Abstract. The UKIRT JHK-band spectrum of GRS 1915+105 shows strong He I (2.059 μm) and Brγ (2.166 μm) emission lines. Eikenberry et al. (1998) found flux variations of a factor of 5 in these lines on a 5 min timescale. Based on the detection or not of the He II emission line, it was suggested that the companion could be a LMXB or a HMXB, respectively. Since the spectral type of the companion star of GRS 1915+105 is still an open question we attempt to clarify the issue by revisiting the object and comparing the JHK spectrum with that of the Be star DM +49 3718 and the prototype X-ray binary Sco X-1.

Keywords: spectroscopy, GRS 1915+105, black hole candidates

1. Introduction

We obtained JHK-band spectra of the X-ray binary GRS 1915+105 (Castro-Tirado et al. 1994) at the 3.8m UKIRT (+ CGS4) on Mauna Kea during the night of 1999 July 8. We also obtained JHK spectra of Sco X-1 and the Be star DM +49 3718 in order to compare them with the spectral slope and emission line properties of GRS 1915+105. The spectra were bracketed by observations of nearby F-type stars, used during the data reduction to remove the telluric atmospheric features.

2. Observations and Results

GRS 1905+105 is not a Wolf-Rayet star, like Cyg X–3 (van Kerkwijk et al. 1992), since we detect Brγ in emission (see also discussion in Castro-Tirado, Geballe and Lund 1996) but no absorption features from the companion star (neutral lines or molecular bands), as seen in GX 1+4 (Bandyopadhyay et al. 1997). There is no trace of He II emission line at a time when the radio spectrum was flat and thus the

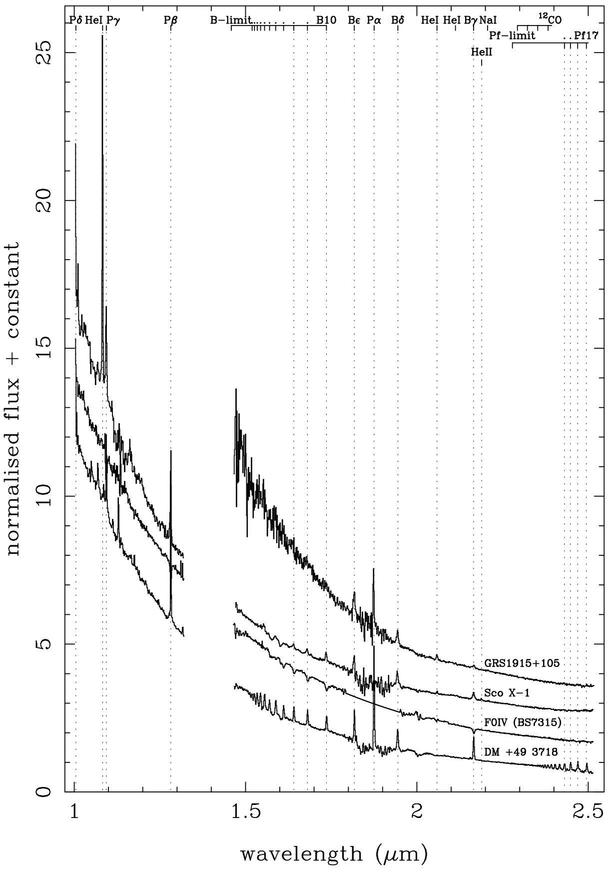

Figure 1. The deredenned HK spectrum of the microquasar GRS 1915+105 and the JHK spectra of Sco X-1 and the Be star DM +49 3718. Also plotted is the JHK spectrum of the F0IV star BS 7315. The spectra have been normalised by dividing by the flux at 2.250 μm and then offset on the y-axis by adding a multiple of 1 to each spectrum.

disc was close to quiescence. The last flaring activity was observed on 1999 July 2. The radio and X-ray continua were in their lowest states which indicate that the accretion disc was very quiet on 1999 July 8 (Martí et al. 2000). It is unclear if the He II emission is produced along the jet, in the accretion disc or on the companion star. However, the X-ray burst activity is related to the jet/disc system centred on the compact object (Belloni et al. 1997), rather than the companion star, and thereafter is the most likely cause for pumping up the transient He II emission. This hypothesis is supported by the absence of He II emission during quiescence, which is the time that the inner disc is being replenished by gas, suggesting that the X-ray luminosity is not sufficient to pump up the He II line through photoionization of the accretion disc. There is Na I doublet emission (2.206 and 2.209 μm) with an equivalent width of –2.6±1.3 Å and a trace of He I emission at 2.113 μm. However, the spectrum of GRS 1915+105 is different from that of the Be star DM +49 3718 in that only a few H lines are visible, which have larger velocity widths and smaller equivalent widths, in addition to the helium emission. We dereddened the GRS 1915+105 spectrum using E(B–V)=9.6 (Boër et al. 1996), and A_V/E(B-V) = 2.76 so A_V=26.5 (Chaty et al. 1996) and the extinction law from Howarth (1983). There was insufficient signal in the J-band, given the large extinction, though after smoothing it was possible to combine the J-band spectrum with the H and K-band spectra to derive a power law index of –5.15±0.02. The power-law suggests that the radiation increases towards to J. The steeper slope in GRS 1915+105 than in the Be star DM +49 3718 indicates that either the dereddening is wrong or that there is a significant J-band emission: from the binary components, disc or a star, or from an unknown contributor (or from both). Morevover, during flares the dominant IR component is due to synchrotron emission (Fender and Pooley 1998, Mirabel et al. 1998) and it is possible that such emission could persists at a much lower level during the quiescence.

3. Conclusions

Our comparison of the IR spectra of the microquasar GRS 1915+105, the prototype X-ray binary Sco X-1 and the Be star DM +49 3718 give the following results:

- The spectral characteristics of the Be star differ from those of Sco X–1 and GRS 1905+105.
- The main difference between the Sco X–1 and GRS 1915+105 spectra is the He II line at 2.189 μm. In Sco X–1, the He II line is persistent and is most likely related to irradiation of the accretion disc around the compact object. In GRS 1915+105, the He II emission line is transient and is observed only during the X-ray bursting activity.
- The other difference between the Sco X–1 and GRS 1915+105 K-band spectra is the weaker He I line at 2.058 μm, which indicates a higher luminosity class for the donor star to GRS 1915+105.

A more detailed discussion can be seen in Harlaftis, Dhillon and Castro-Tirado (2001). These results are also consistent with the identification of the donor as a late-type star by Greiner et al. (2001).

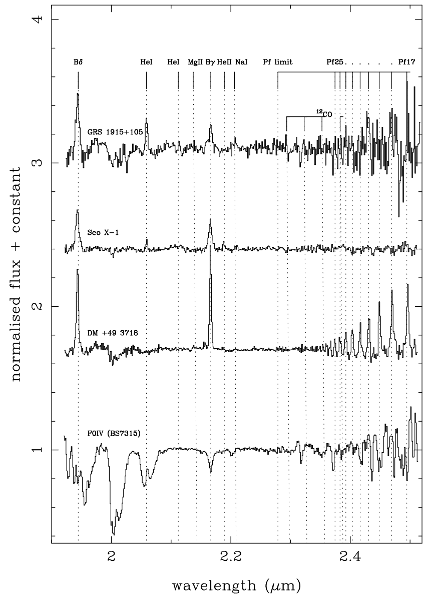

Figure 2. The K-band spectra of the microquasar GRS 1915+105, Sco X-1, and the Be star DM +49 3718. Also plotted is the K-band spectrum of the F0IV star BS 7315 which indicates the location of telluric absorption features. Note the weak He II and Na I doublet emission lines in the X-ray binary spectra. The spectra have been normalized by dividing by a spline fit to their continua and then offset on the y-axis by adding a multiple of 0.7 to each spectrum.

References

Bandyopadhyay R., Shahbaz T., Charles P. A., van Kerkwijk, M. H., Naylor T., 1997, MNRAS, 285, 718

Belloni T., Méndez M., King A. R., van der Klis M., van Paradijs J., 1997, ApJ 479, L145

Boër M., Greiner J., Motch C., 1996, A&A, 305, 835

Castro-Tirado A. J., Brandt. S., Lund N., 1994, ApJS, 92, 469

Castro-Tirado A. J., Geballe T. R., Lund N. et al., 1996, ApJ, 461, L99

Chaty S., Mirabel I. F., Duc P. -A., Wink J. E., Rodriguez L. F., 1996, A&A, 310, 825

Eikenberry S. S., Matthews K., Morgan E. H., Remillard R. A., Nelson R. W., 1998, ApJ, 494, L61

Fender, R. P. and Pooley, G. G. 1998, MNRAS 300, 573

Greiner, J., McCaughrean, M. J., Cuby, J. G., Castro-Tirado, A. J., Mennickent, R. 2001, These Proceedings

Harlaftis, E., Dhillon, V. S. and Castro-Tirado, A. J., 2001, A&A, in press

Howarth I. D., 1983, MNRAS, 203, 301

Martí J., Mirabel I F., Chaty S., Rodríguez L F., 2000, A&A, in press

Mirabel I. F., Dhawan V., Chaty S., Rodríguez L. F., Martí J., Robinson C. R., Swank J., Geballe T. R., 1998, A&A 330, L9

van Kerkwijk M. H., Charles P. A., Geballe T. R., et al., 1992, Nature, 355, 703

On the Mass-Donating Star in GRS 1915+105

Stephen S. Eikenberry
Cornell University

Reba M. Bandyopadhyay
NRL/NRC

Abstract. Geometric constraints and the lack of eclipses in GRS 1915+105 are used to place limits on the mass of the companion star. We rule out any companion with $M_s > 19.4 M_☼$ for a black hole mass of $M_{BH} \simeq 30 M_☼$

Keywords: X-ray:stars, black hole physics, GRS 1915+105, close binaries

We present an analysis of constraints on the companion mass for the Galactic microquasar GRS 1915+105. Using the known inclination angle and stability of the jet axis, we can rule out massive ($M_s > 3M_☼$) companions with orbital axes not aligned with the jet axis. For an aligned orbital axis, we constrain the ratio of the stellar radius to the binary semi-major axis to be $R_s/a < 0.342$, based on the lack of X-ray eclipses. We then show that these constraints together with the X-ray luminosity, approximate black hole mass, and observations of the X-ray absorbing column density towards GRS 1915+105 rule out accretion via stellar wind from a massive companion, implying that accretion occurs via Roche-lobe overflow. In that case, the constraint on R_s/a rules out any companion with $M_s > 19.4M_☼$ for a black hole mass of $M_{BH} \simeq 30M_☼$. The lack of significant X-ray reprocessing in the infrared from GRS 1915+105 also provides constraints on the mass and temperature range of a Roche-lobe-filling mass donor.

These results are inconsistent with the massive companion claimed by Marti et al. (2001), but mesh well with the results of Greiner et al. (2001).

References

Marti, J., et al. 2001, these proceedings
Greiner, J., et al. 2001 these proceedings

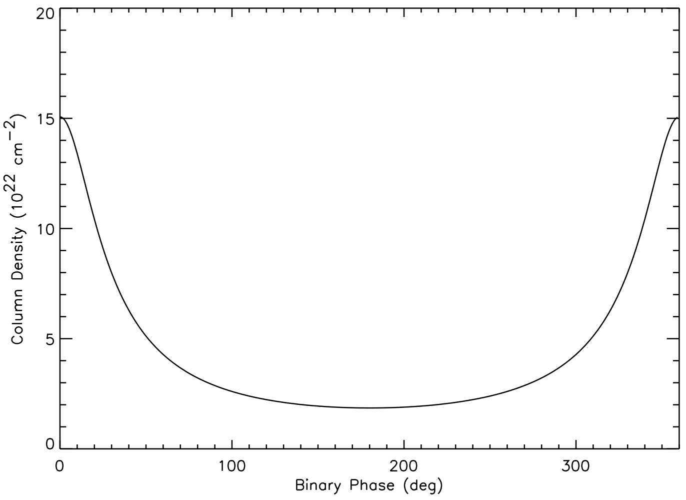

Figure 1. Orbital variation of observed X-ray absorption column density for wind-fed accretion from an LBV-type star. Assumes $\dot{M} = 2.65 \times 10^{-5}\ M_{\odot}\ \mathrm{yr}^{-1}$, $a = 2.9$ AU, and $v_{wind} = 10^3 \mathrm{kms}^{-1}$. Note that both the maximum amplitude of the absorption and its strong variations are inconsistent with observations of GRS 1915+105.

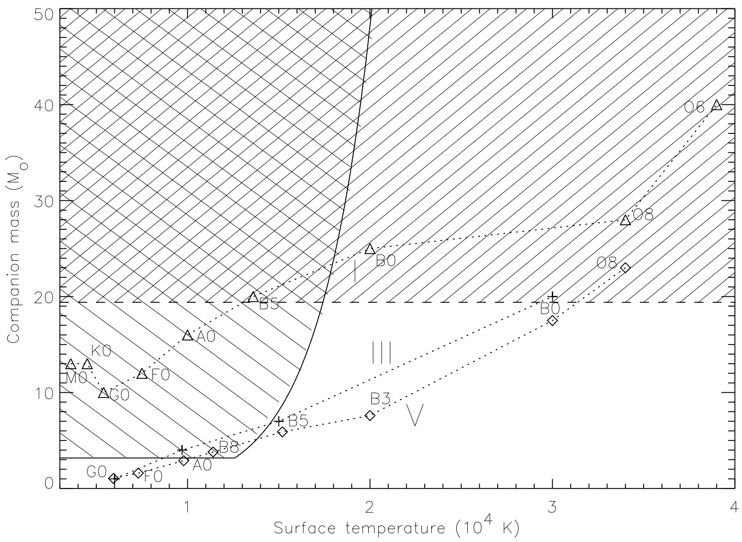

Figure 2. Constraints on mass and temperature for stars donating mass via Roche-lobe overflow. The hatched areas are regions which are ruled out by: (i) the limit on R_s/a (bounded by horizontal dashed line); (ii) limits on X-ray reprocessing (bounded by solid curve); (iii) the limit on $q > 0.1$ (allowing all stars with $M < 3M_{\odot}$). Roman numerals indicate stellar luminosity class for supergiant (I), giant (III), and main-sequence (V) stars. Assumes $M_{BH} = 30M_{\odot}$.

Recent *Hubble Space Telescope* Results on X-Ray Novae

R. I. Hynes (rih@astro.soton.ac.uk)
Department of Physics and Astronomy, University of Southampton, Southampton, SO17 1BJ, UK

C. A. Haswell and S. Chaty
Department of Physics and Astronomy, The Open University, Walton Hall, Milton Keynes, MK7 6AA, UK

C. R. Shrader
Laboratory for High-Energy Astrophysics, NASA Goddard Space Flight Center, Greenbelt, MD 20771, USA

W. Cui
Department of Physics, Purdue University, West Lafayette, IN 47907, USA

C. W. Mauche
Lawrence Livermore National Laboratory, L-43, 7000 East Avenue, Livermore, CA 94550, USA

Abstract. *RXTE* has recently discovered two new optically bright black hole candidates (BHCs): XTE J1859+226 and XTE J1118+480. We observed both with *HST*/STIS, the first outburst observations of X-ray novae with this instrument. We followed broad band spectral evolution, detected correlated X-ray/UV rapid variability and performed high resolution UV spectroscopy. We present a summary of initial results on the spectral energy distributions observed.

XTE J1859+226 is a classical X-ray nova showing an exponential decay lightcurve and quasi-periodic oscillations typical of BHCs (Cui et al. 2000). The STIS/G230L spectrum defines the 2175 Å interstellar absorption feature $\Rightarrow E(B-V) = 0.58 \pm 0.07$. Hence we deredden the spectra to obtain the intrinsic SED. Early in the outburst SEDs are well fitted by a simple irradiated disc model ($T \propto R^{-3/7}$, Vrtilek et al. 1990). The edge temperature, $T_{\rm out}$, remains constant so the edge of the hot region must move inward as the X-rays decline, possibly due to a cooling wave or self-shielding by the disc. The last spectrum is better fitted by a viscously heated disc model (Shakura & Sunyaev 1973) with $T_{\rm out} \sim 8000$ K as predicted by disc instability models.

XTE J1118+480 lies at high latitude and suffers very little extinction making *EUVE* observations possible. Its unusual outburst only reached the canonical low/hard state of black hole candidates with a very low X-ray to optical flux ratio. Its IR–UV SED shows roughly constant f_ν (Hynes et al. 2000). A weak Balmer jump in absorption implies some thermal emission, likely the disc. The spectrum of a disc extending to last stable orbit (A) clearly ruled out but the exact interpretation depends on an uncertain $N_{\rm H}$: Model B has the inner disc at a few

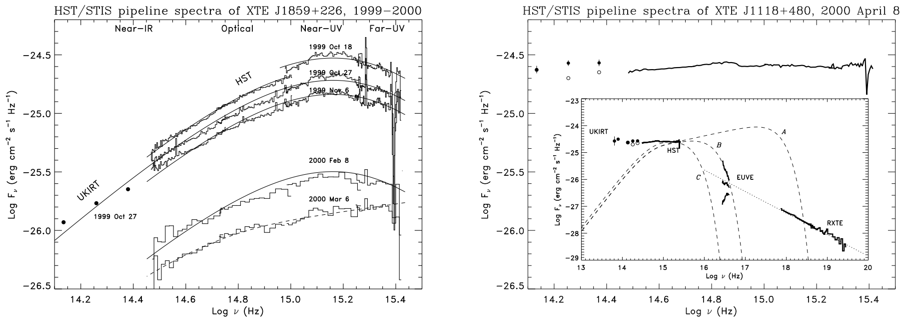

Figure 1. Left: *HST* and UKIRT observations of XTE J1859+226 showing the evolution of the SED through the outburst. Right: SED of XTE J1118+480 on 2000 April 8 from *HST* and UKIRT. Inset also shows simultaneous *RXTE* and *EUVE* data. Note that both plots use the same axes, so the shape of the SEDs can be directly compared.

hundred $R_{\rm s}$, consistent with thermal EUV if $N_{\rm H} = 1.0 \times 10^{20}\,{\rm cm}^{-2}$. Model C has the inner disc at a few thousand $R_{\rm s}$ and works if $N_{\rm H} = 0.75 \times 10^{20}\,{\rm cm}^{-2}$ and the EUV is non-thermal. The X-ray power-law is likely non-thermal, and has a spectral index typical of the low/hard state. A disc model cannot explain the flatness of the IR spectrum so another low energy component, likely synchrotron emission, is needed; see also contributions by Fender et al. and Markoff et al. for discussion of this component.

Acknowledgements

This work was supported by grant F/00-180/A from the Leverhulme Trust and is based on observations with the NASA/ESA *Hubble Space Telescope*, obtained at STScI, operated by AURA under NASA contract NAS5-26555. *EUVE* observations were made possible by a generous grant of Director's Discretionary Time. UKIRT is operated by the JAC on behalf of the UK PPARC. Thanks to the staff at these facilities.

References

Cui, W., Shrader, C.R., Haswell, C.A., Hynes, R.I.: 2000, ApJ, 535, L123
Hynes, R.I., Mauche, C.W., Haswell, C.A., Shrader, C.R., Cui, W., Chaty, S.: 2000, ApJ, 539, L37
Shakura, N.I. & Sunyaev, R.A.: 1973, A&A, 24, 337
Vrtilek, S.D., Raymond, J.C., Garcia, M.R., Verbunt, F., Hasinger, G., Kurster, M., 1990: A&A, 235, 162

The moderate and high-speed photometry of the newly discovered black hole candidate X-ray transient XTE J1118+480 *

Elena P. Pavlenko†, Elena S. Dmitrienko, and Nikolai M. Shakhovskoi
Crimean Astrophysical Observatory, Naychny , Crimea, Ukraine
(`pavlenko@crao.crimea.ua`*),*

Sergei Yu. Shugarov,, Nataly A. Katysheva, and Igor M. Volkov
Sternberg Astronomical Institute, Moscow State University, Universitetskii pr. 13, Moscow, 119899 Russia (`shugarov@sai.msu.ru`*)*

Abstract. Our March–May photometry of XTE J1118+480 during the plateau of outburst confirmed the existence of the known 0.17085d variations in R with amplitude $0^m.06$ and the 10-s QPOs, which are stronger in I band.

Keywords: close binaries, X-ray novae, XTE J1118+480

We observed XTE J1118+480 in 2000 from the end of March during 23 nights in the R band at the SAI Zeiss-600 and CrAO 38-cm Cassegrain telescopes in Crimea with a SBIG CCD ST-7 camera, and at the Zeiss-300 cm telescope of the Students SAI Observatory in Moscow. These observations have been carried out with exposure times of several tens of seconds. High-speed UBRI photometry was made at the CrAO AZT-11 1.25m telescope on April, 30 with 2-s and May, 15 with 5-s exposure times. During the first 45 days after the March outburst XTE J1118+480 has shown no prominent brightness decline (Fig. 1, top panel of left part). The plateau-like shape of the outburst maximum lasted $\sim 100d$ and then changed to a rapid fading. A similar behaviour was seen in A0620–00 (Shugarov 1976) and GRO J0422+32 (Chevalier and Ilovaisky, 1995).

We confirm the existence of $0.17085d$ light variations (Cook et al. 2000; see Fig. 1, middle and bottom panels of left part), and also confirm the 10-s QPOs (Patterson et al. 2000) which we found to be more prominent in the I band. On the right part of Fig. 1 the power spectra for the two runs of of the observations are given. The main peak is split between 9.08 s and 10 s. This may be caused by a change of these QPOs during two weeks.

* The work is partially supported by the RFBR grants RFBR NN 00-15-96553, 00–02–16471 and 99-02-17589

† EPP is thankful to Instituto de Astrofisica de Andalucia for supporting her visit to Granada.

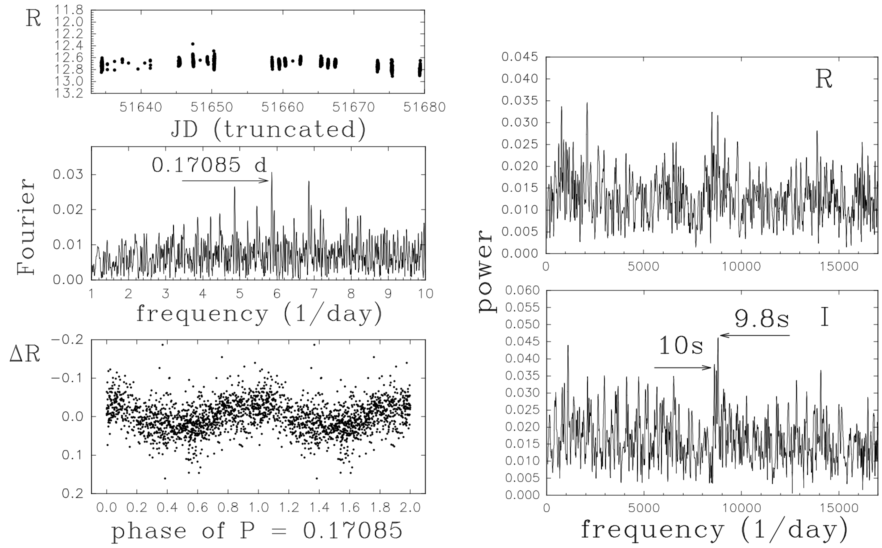

Figure 1. **Left:** Top panel: The behaviour of XTE J1118+480 at outburst maximum; middle panel: The power spectrum for all data; the arrow indicates the most significant period at 0.17085 days; bottom panel: Data, folded on this period. **Right:** The summed power spectra in R and I for data obtained on 30.04 and 15.05, 2000

References

Shugarov, S. X-Nova V616 Monocerotis (A0620-00) *Var.Star.*, 20: 251–254, 1976.

Chevalier, C. and Ilovaisky, S.A. CCD photometry of GRO J0422+32 during activity and quiescence *Astron. Astrophys.*, 297: 103–, 1995.

Cook, L., Patterson, J., Buczinski, D. et al. *IAU Circ.*, 7397, 2000.

Patterson, J., Fried, R., Harvey, D. et al *IAU Circ.*, 7412, 2000.

Superhumps in Black Hole X-Ray Transients *

C.A. Haswell (c.a.haswell@open.ac.uk), D.J. Rolfe,
Department of Physics and Astronomy, The Open University,

A.R. King, J.R. Murray,
Department of Physics and Astronomy, Leicester University,

P.A. Charles
Department of Physics and Astronomy, University of Southampton

Abstract. The superhumps in black hole X-ray transients result from a modulation in the area of the accretion disc. We discuss implications of this for parameter determinations in LMXBs.

1. Introduction

Superhumps are a periodic photometric modulation with period $P_{\rm sh}$ slightly longer than $P_{\rm orb}$. They were discovered in extreme mass-ratio cataclysmic variables (CVs) harbouring eccentric accretion discs performing apsidal precession (Warner, 1995). CV superhumps are powered by tidally-driven modulations in viscous dissipation (Murray, 2000). Many black hole X-ray transients (BHXRTs) satisfy the extreme mass-ratio requirement for the development of an eccentric disc (Haswell et al, 2000; Whitehurst & King, 1991) and several (*e.g.* GS 1124–68, GRO J0422+32) have shown superhumps (O'Donoghue & Charles, 1996; Uemura et al, 2000).

The optical light in X-ray bright LMXBs is dominated by reprocessing: the optical emission from viscous dissipation is smaller by a factor of $\sim 10^{-3}$. This means superhumps in BHXRTs cannot be powered in the same way as those in CVs (Haswell et al, 2000).

2. The Mechanism Powering LMXB Superhumps

Recently, eclipse mapping of V348 Pup, a superhumping CV, revealed clear evidence that the spatial distribution of the disc emission is modulated on $P_{\rm sh}$ (Rolfe, Haswell, & Patterson, 2000). Numerical simulations of a precessing eccentric disc in an extreme mass ratio binary (Murray, 2000) reveal a modulation in shape on $P_{\rm sh}$ (Haswell et al, 2000). Figure 1 shows a $\sim 10\%$ modulation in the area of the disc. This will clearly modulate $L_{\rm opt}$, as $L_{\rm opt} \propto A_{\rm eff} L_X$.

* This work was supported by grant F/00-180/A from the Leverhulme Trust.

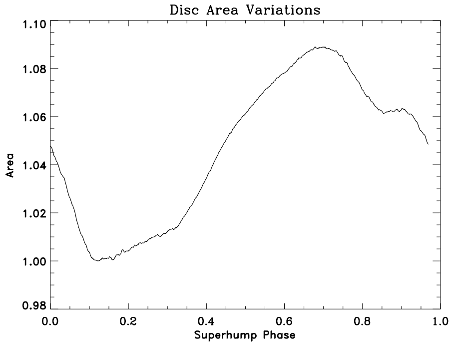

Figure 1. Disc surface area as it varies over the course of a single superhump cycle.

3. Implications

Superhumps occur only if the disc extends out to the radius where $\Omega_{\rm Kep} = 3\Omega_{\rm orb}$; this requires an extreme mass ratio. For neutron star LMXBs, superhumps consequently require $P_{\rm orb} < 4.2$hr. For a black hole accretor there is no clear restriction on mass, so superhumps are not restricted to short $P_{\rm orb}$. Thus we can infer black hole primaries for superhumping LMXBs with $P_{\rm orb} > 4.2$hr and main sequence mass donors (Haswell et al, 2000).

The mass donor star also reprocess X-rays. Consequently, the modulation in disc shape is likely to cause the most prominent superhump modulation when the disc is viewed face-on. At higher inclinations the disc reprocessing area, $A_{\rm eff}$, is foreshortened, diminishing the superhump modulation, while the orbital modulation due to the changing aspect of the mass donor will be increased. The disc shape modulation probably includes changes in vertical structure. For systems which are viewed edge-on, this may lead to modulations in occultation of the central emitting regions. X-ray dips attributed to such occultation are observed in several LMXBs. These dips have been used to infer $P_{\rm orb}$, but they may be modulated at $P_{\rm sh}$ or the disc precession period.

References

Haswell, C.A., King, A.R., Murray, J.R., Charles, P.A. 2000, *MNRAS*, in press. astro-ph/0008367.

Murray, J.R., 2000, *MNRAS*, 314, L1. astro-ph/9911466.

O'Donoghue D., Charles P.A., 1996, *MNRAS*, 282, 191.

Rolfe, D.J., Haswell, C.A., Patterson, J. 2000, *MNRAS*, 317, 759.

Warner B. 1995, Cataclysmic Variable Stars, Cambridge Univ. Press, Cambridge.

Whitehurst R., King A.R. 1991, *MNRAS*, 249, 25

Uemura, M. et al 2000, IAU Circ 7418

XTE J1550−564: A superluminal ejection during the September 1998 outburst

Diana Hannikainen
Department of Physics & Astronomy, University of Southampton, Southampton SO17 1BJ, UK

Duncan Campbell-Wilson, Richard Hunstead, Vince McIntyre*
School of Physics, University of Sydney, NSW 2006, Australia

Jim Lovell, John Reynolds, Tasso Tzioumis
ATNF, CSIRO, PO Box 76, Epping, NSW 1710, Australia

Kinwah Wu†
MSSL, University College London, Holmbury St. Mary, Dorking, Surrey, RH5 6NT, UK

Abstract. In 1998 September, the X-ray transient XTE J1550−564 underwent a major outburst in soft and hard X-rays, followed by a radio flare. Australian Long Baseline Array images obtained shortly after the peak in the radio flare showed evolving structure. The components observed have an apparent separation velocity of $> 2c$.

Keywords: XTE J1550−564, radio continuum:stars

1. Introduction

The X-ray transient XTE J1550−564 was discovered simultaneously by the All-Sky Monitor on the Rossi X-ray Timing Explorer (Smith, 1998) and by the Burst and Transient Source Experiment on the Compton Gamma-Ray Observatory (Wilson et al., 1998) on MJD 51063 (1998 Sept 7; MJD=JD−240000.5). Following the discovery of the radio counterpart (Campbell-Wilson et al., 1998), XTE J1550−564 was monitored with the Molonglo Observatory Synthesis Telescope (MOST) at 843 MHz between MJD 51065 and 51092. A flare was recorded, peaking with an estimated flux density of 380 mJy on MJD 51078. Two Very Long Baseline Interferometry (VLBI) observations using the Australian Long Baseline Array (LBA) were performed 2–3 days after the MOST flare. In this paper we present the resulting images from these observations, and discuss briefly the implications of the evolving structure observed.

* Present address: ATNF, CSIRO, PO Box 76, Epping, NSW 1710, Australia
† Permanent address: School of Physics, University of Sydney, NSW 2006, Australia

Table I. VLBI Observations

Date	T_{start} (UT)	T_{end} (UT)	Antenna	Frequency (GHz)
1998 Sept 24	02:17	06:08	DSS45 (34m)	2.29 & 8.4
Mid-point (MJD):	51080.7		Hobart (26m)	2.29 & 8.4
			Mopra (22m)	2.29
1998 Sept 25	22:30	09:00	DSS43 (70m)	2.29 & 8.4
Mid-point (MJD):	51081.7		Hobart (26m)	2.29 & 8.4
			Mopra (22m)	2.29
			ATCA (6×22m)	2.29

Table II. Flux densities at 2.29 GHz

	Flux density (mJy)			
Date	East	Central	West	Total
1998 Sept 24	71	–	20	91
1998 Sept 25	19	25	8	52

2. Observations and results

The VLBI observations were carried out on 1998 Sept 24 and 25 and are summarized in Table I. The data post-correlation used the AIPS task FRING to find fringes and calibrate the fringe amplitude. Due to the small number of baselines, the Caltech program DIFMAP was used to model and source fit the data, and measure the flux densities.

Figure 1 shows the resulting VLBI images at 2.29 GHz from 1998 Sept 24 in the top panel and from 1998 Sept 25 in the bottom panel. Phase-referenced observations were not performed on either day so the zero coordinate in the images is arbitrary. The flux densities (with uncertainties of 10–20%) of the components are summarized in Table II.

The image from 1998 Sept 25 clearly shows an additional component compared to the image on 1998 Sept 24. As the image center is arbitrary, it is not obvious how to relate the components seen in the two images. However, two-point spectral indices derived from Australia Telescope Compact Array data at the time of the radio flare show a flattening just prior to the first VLBI observation from about $\alpha = -0.45$ to -0.1 ($S_\nu \propto \nu^\alpha$) over the interval 4.8–8.6 GHz (Hannikainen et al., 2000a). This is very similar to the behavior seen in the 4.8–8.6 GHz

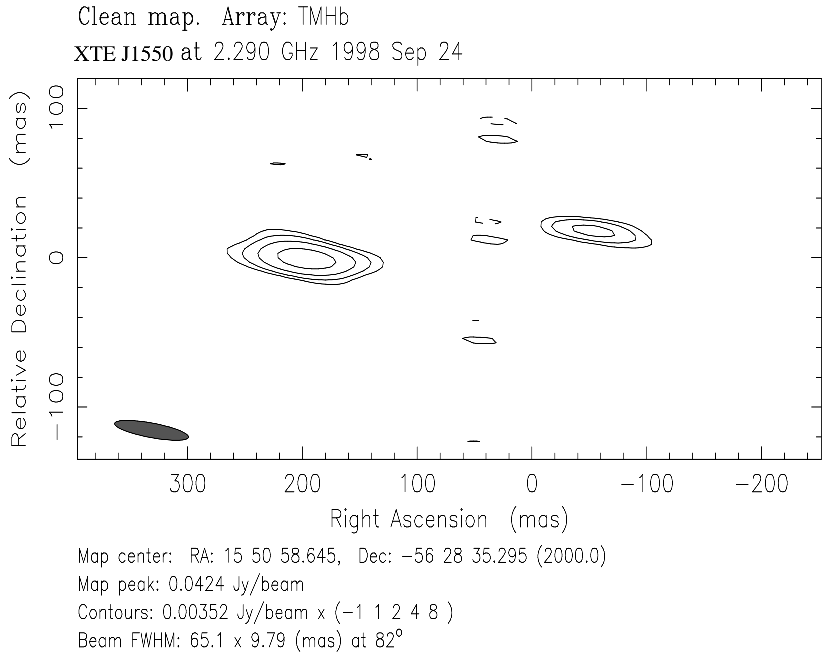

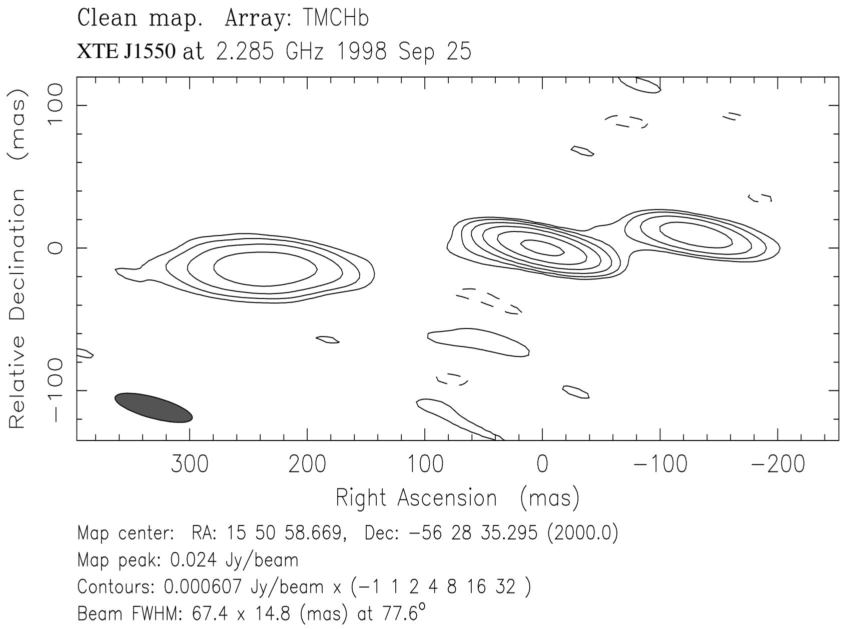

Figure 1. VLBI images at 2.29 GHz from 1998 Sept 24 (MJD 51080.7, top) and 1998 Sept 25 (MJD 51081.7, bottom). The zero coordinate is arbitrary. The beam is shown in the lower left-hand corner in each image.

two-point spectral index of GRO J1655−40 during the 1994 jet ejection episodes (Hannikainen et al., 2000b) and strongly suggests that a new optically thick outburst occurred. If this interpretation is correct, then we associate the central component in the bottom panel with the flaring core and thus the two components in the top panel, the ejecta, can be associated with the two outermost components in the bottom panel. This interpretation is reinforced by the 1998 Sept 25 single-baseline 8.4 GHz data which shows a new unresolved component not present in the 1998 Sept 24 data. This means that in one day the ejecta have moved apart by approximately 115 mas. At an estimated distance of 3.5–5 kpc (McIntyre, in preparation) this implies a separation velocity $> 2c$ for the ejecta, which makes XTE J1550−564 the fifth Galactic source to exhibit apparent superluminal motion.

3. Conclusions

We have presented two VLBI images of XTE J1550−564 from the time of the 1998 September outburst and showed that the source evolved over a period of 24 hours. The two outermost components seen in the 1998 Sept 25 image are associated with the two components in the 1998 Sept 24 image, implying an apparent separation velocity of $> 2c$.

Acknowledgements

The Australia Telescope Compact Array and the Mopra Telescope are part of the Australia Telescope which is funded by the Commonwealth of Australia for operation as a National Facility managed by CSIRO. We thank the staff of both the University of Tasmania, Hobart, and the Canberra Deep Space Communications Complex, Tidbinbilla. DH acknowledges the support of a PPARC postdoctoral research grant to the University of Southampton.

References

Campbell-Wilson, D., McIntyre, V., Hunstead, R., and Green, A.: 1998, *IAUC* 7010
Hannikainen, D., Wu, K., Campbell-Wilson, D., Hunstead, R., Lovell, J., McIntyre, V., Reynolds, J., and Tzioumis, T.: 2000a, submitted to *Proceedings of the 4th INTEGRAL Workshop*, ESA-SP
Hannikainen, D.C., Hunstead, R.W., Campbell-Wilson, D., Wu., K., McKay, D.J., Smits, D.P., and Sault, R.J.: 2000b, *ApJ*, 540, 521
Smith, D.A.: 1998, *IAUC* 7008
Wilson, C.A., Harmon, B.A., Paciesas, W.S., and McCollough, M.: 1998, *IAUC* 7010

Optical behaviour of XTE J1859+226 and XTE J1550–564 from outburst to quiescence

C. Sánchez-Fernández (celia@ laeff.esa.es)
LAEFF-INTA, Madrid (Spain)

A. J. Castro-Tirado and A. Giménez
IAA-CSIC, Granada (Spain) and LAEFF-INTA, Madrid (Spain)

C. Zurita and J. Casares
IAC, Tenerife (Spain)

Abstract. We present here the optical light curves of the Soft X-ray Transients XTE J1550-564 and XTEJ1859+226 from outburst to quiescence

Keywords: X-ray transient, black hole candidates

1. XTE J1550-564

XTE J1550-564 was first detected on Sep. 7.09 UT 1998 by the All-Sky Monitor on RXTE (Smith & Remillard 1998). This object is the brightest SXT yet detected by RXTE The source was also detected in hard X-rays (20-100 keV) by BATSE/CGRO (Wilson et al. 1998). On the basis of its timing and spectral properties in X-rays (Cui et al. 1999; Wijnands et al. 1999) the source was classified as a black hole candidate. An optical counterpart with V$\sim$ 16 mag. was proposed by Orosz et al. (1998). This object was confirmed as the optical counterpart by means of a 300-s optical spectrum which displayed prominent H_α emission as well as broad and weaker emission lines from H_β and HeII (Castro-Tirado et al. 1998, Sánchez-Férnandez et al. 1999). Radio emission from the source was also detected (Campbell-Wilson et al. 1998).

Fig. 1 displays the optical light curve of XTE J1550-564 based on our measurements. Public ASM X-ray data as well as optical data from IAU Circulars have been included for completeness.

1.0. The October 1998 outburst

The soft X-rays light curve is characterized by a gradual brightening, a giant flare, which is also detected in optical wavelengths, a post-flare plateau ($\sim$25 days) and a subsequent decay. Amazingly, the optical emission does not follow the same pattern and the plateau phase is not present. The optical decay phase takes place just after the flare, with decay rates $\sim$ 0.045 mag./day (Sánchez-Fernández et al. 1999).

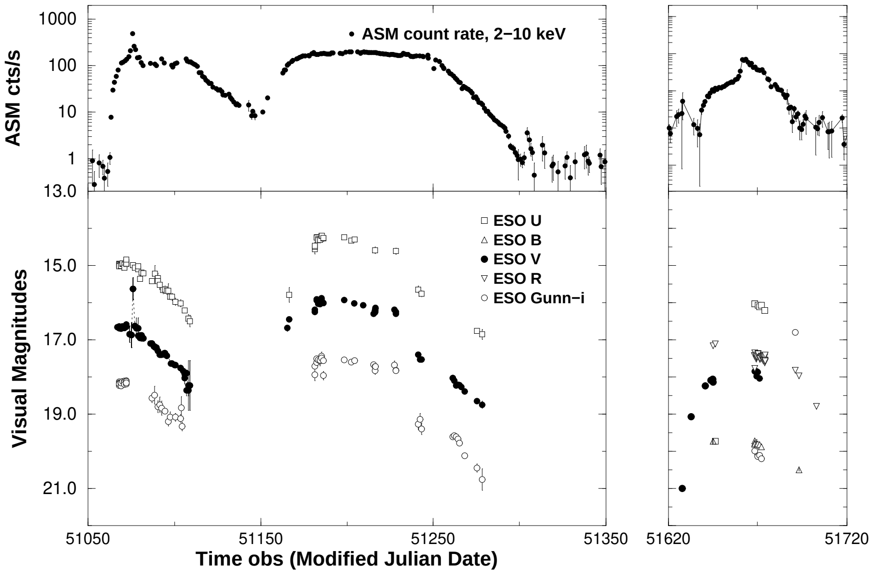

Figure 1. Optical/X-rays light curves of XTE J1550-564 showing the three outbursts referred in the text.The quiescent phase between the second and third outbursts has been omitted for clarity.

1.0. The 1998/1999 outburst

By the end of 1998, when the source appeared to be heading towards quiescence, it experienced a prolonged reflare which was observed at X-ray and optical wavelengths, and which lasted for about 6 months (Jain et al. 2000, Sánchez-Fernández et al. 2000; see fig. 1). In this reflare, a new plateau appeared, both in soft X-rays and optical wavelengths, though with different durations ($\sim$ 75 days in soft X-rays; $\sim$ 50 days in optical). The optical decay rates are $\sim$ 0.053 mag./day.

1.0. The April 2000 outburst

After this secondary outburst, the source stayed in quiescence for about one year until it experienced a minor outburst in April, 2000 (Smith et al. 2000). Stochastic flaring activity was observed during this outburst but no convincing evidence for the orbital period was found. An optical spectrum displaying emission lines characteristic of SXTs in outburst was obtained during this same epoch (Sánchez-Fernández et al. 2000).

2. XTE J1859+226

XTE J1859+226 was first detected on Oct. 9.658 by ASM/RXTE (Wood et al. 1999) at an intensity of 160 ± 15 mCrab (2-12 keV). On the basis of its timing and spectral properties in X-rays, the source was classified as a black hole candidate (see for example Markwardt et al. 1999). The optical counterpart was soon discovered by Garnavich et al. (1999). A likely radio counterpart to the X-ray transient was also detected (Pooley et al. 1999).

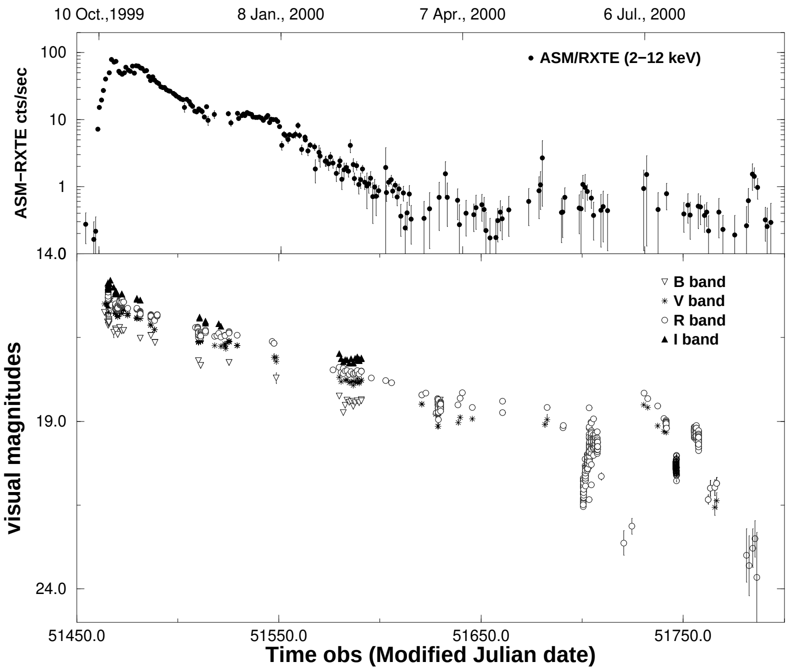

Figure 2. Optical/X-rays light curves of XTE J1859+226 from outburst to quiescence. Soft X-ray data have been obtained from RXTE public archive.

We present in Fig. 2 the optical light curve of XTE J1859+226 based on our measurements. Public ASM X-ray data as well as optical data from IAU Circulars have been included for completeness.

The optical and soft X-rays light curves display the typical Fast Rise + Exponential Decay (*FRED*) shape, with rise-time (10%-90% peak) of ∼ 5 days in ASM data and an e-fold time of ∼ 23 days. The initial decay rate observed in optical is ∼ 0.018 mag./day. A secondary maxima is detected both in ASM and optical light curves ∼ 55 days after primary outburst. This secondary maxima should be due to a new injection of matter in the accretion disk as a response from the secondary star to x-ray heating. In addition, the optical light curve shows some additional peculiarities. Namely, a fast decay from R$\sim$19 to 21.5 mag. 235 days after the extrapolated onset of outburst (Casares et al. 2000), followed by 3 minioutbursts (see Zurita et al. 2001). There is no evidence of minioutuburst in the ASM light curve so an explanation based on X-ray reprocessing to these phenomena should be ruled out (see Zurita el al. 2000 for a futher discussion).

2.0. Evidences of an outside-in outburst

By carefully examining the light curve at the begining of outburst we find evidences that the optical light curve had already peaked while the soft X-rays light curve wa1s still in the rising phase. This behaviour has also been observed in some other SXTs (Aql X-1, GRO J1655-40, XN 2023+338, GRS 1124+68 and GRO J0422+32) and is thought to be the signature of an 'outside-in' outburst, in which a thermal instability in the disk propagates inward. See Zurita el al. (2000) for a futher discussion.

References

Campbell-Wilson, D., McIntyre, V., Hunstead, R., Green, A., Wilson, R. B., Wilson, C. A.: 1998 *IAU Circular* 7010,

Casares, J., Rodrigues, P., Zurita, C., Shahbaz, T., Charles, P., Hynes, R., Abbott, T., Hakala, P.: 2000 *IAU Circular* 7451,

Castro-Tirado, A. J., Duerbeck, H. W., Hook, I., Yan, L.: 1998 *IAU Circular* 7013,

Cui, W., Zhang, S. N., Chen, W., Morgan, E. H.: 1999 *ApJ* Vol. 512., p.793

Jain, R. K., Bailyn, C., Orosz, J. A., McClintock, J. E., Sobczak, J. E.,Remillard, R.: 2000 *Accepted for publication in ApJ*

Garnavich, P. M., Stanek, K. Z., Berlind, P.: 1999 *IAU Circular* 7269,

Markwardt, C. B., Marshall, F. E., Swank, J. H.: 1999 *IAU Circular* 7274,

Orosz, J., Bailyn, C., Jain, R.: 1998 *IAU Circular* 7009,

Pooley, G. G., Hjellming, R. M.: 1999 *IAU Circular* 7278,

Remillard, R., Morgan, E., McClintock, J., Sobczak, G.: 1998 *IAU Circular* 7219,

Sánchez-Fernández, C. Castro-Tirado, A. J., Duerbeck, H. W., Mantegazza, L., Beckmann, V. et al.: 1999 *A&A* Vol. 348L., p. 9

Sánchez-Fernández, C. Zurita, et al.: 2000 *in preparation*

Smith, D. A. and Remillard R.: 1998 *IAU Circular* 7008,

Smith, D. A.; Levine, A. M.; Remillard, R.; Fox, D.; Schaefer, R.; RXTE/ASM Team: 2000 *IAU Circular* 7399,

Wijnands, R., Homan, J., van der Klis, M.: 1999 *ApJ* Vol. 526, p. 33

Wilson, C. A., Harmon, B. A., Paciesas, W. S., and McCollough, M. L.: 1998 *ApJ* Vol. 517, p. 121

Wood, A., Smith, D. A., Marshall, F. E., Swank, J.: 1999 *IAU Circular* 7274,

Zurita, C., Sánchez-Fernandez, C. et al.: 2000 *in preparation*

Zurita, C., Casares, J., Charles, P., Rodriguez Gil, P., Sánchez-Fernández, C, Castro-Tirado, A., Shahbaz, T., Abbot, T., Hakala, P.: 2001 *these proceedings*

Minioutbursts in XTE J1859+226

C. Zurita, J. Casares, P. Rodriguez–Gil and T. Shahbaz
Instituto de Astrofisica de Canarias (IAC)

P.A. Charles
University of Southampton

C. Sanchez–Fernandez
Laboratorio de Astrofisica Espacial y Fisica Fundamental (LAEFF)

A. Castro–Tirado
Instituto de Astrofisica de Andalucia (IAA)

T. Abbot
Nordic Optical Telescope (NOT)

P. Hakala
Turku University

Abstract. Photometry of the X–ray transient XTE J1859+226, obtained during outburst, showed at least 3 minioutbursts. During the second one, the source exhibited a 0.3 mag modulation with QPO flaring activity during the minimum.

Keywords: black hole physics, close binaries, XTE J1859+226

Fig. 1 compares the overall lightcurve of XTE J1859+226 in R–band and X–rays (2–12 keV), since the Oct. 99 outburst. The R light curve can be classified as *FRED*: 'fast–rise exponential–decay'. A 'glitch' is detected in the exponential decay phase ~160 days after the peak, exactly as in A0620–00 (Tsunemi et al. 1977). We have also detected at least 3 minioutbursts when XTE J1859–226 was approaching quiescence. *Minioutbursts* have only been detected in GRO J0422+32 (Chevalier & Ilovaiski 1995) and GRS 1009–45 (Bailyn & Orosz 1995). The source may have reached the quiescent state from Aug 20.

B-band photometry on July 5, during the second minioutburst, showed a decay of about 0.3 mag for 3 hr. During the minimum, the source exhibited *QPO* flaring activity with 20% amplitude (Fig. 2). We find a period of 21.7±0.6 min, very close to that reported by Hynes et al. (1999). We note that flare activity was also found in an individual night during a *minioutburst* in GRO J0422+32 (Chevalier & Ilovaiski 1995). The flaring ceased when the source returned to its predip level. On July 6, the *QPOs* disappeared and instead the source exhibited a smooth sinusoidal modulation with 0.10 mag amplitude. Assuming that the dip in the July 5 light curve is the primary minimum, it occurs exactly 1.3 days before a previous reported minimum (McClintock et al. 2000).

Therefore the orbital period must be a submultiple. We favor an orbital period of 0.65 days although more data is needed for confirmation.

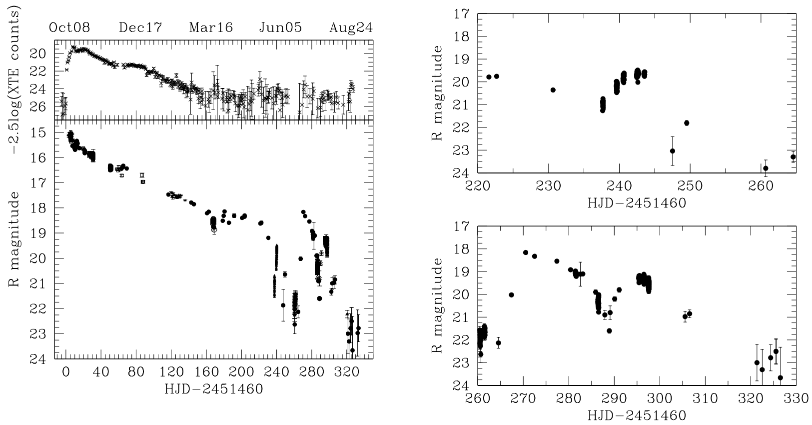

Figure 1. X–Ray and R–band long term light curve of XTE J1859+226 and minioutbursts.

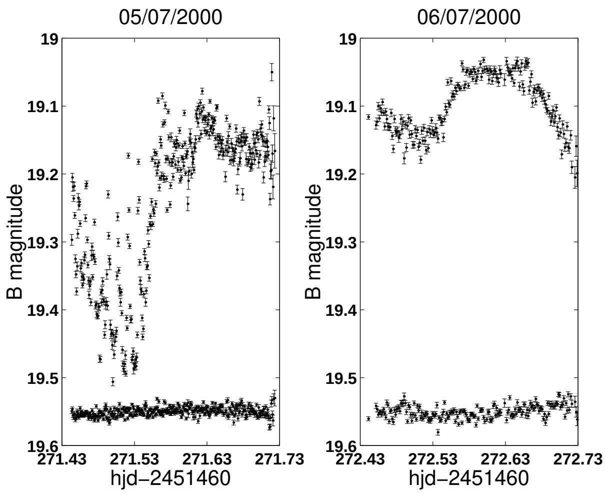

Figure 2. B–band light curves of XTE J1859+226 and comparison star during the second minioutburst

References

Tsunemi, H., Matsuoka, M., Takagishi, K.: 1977, *ApJ* **211**, L15
Chevalier, C., Ilovaiski, S.A.: 1995,*A&A* **297**, pp.103
Bailyn, C.D. & Orosz, J.A.: 1995, *ApJ* **440**, L73
Hynes, R., Haswell, C., Norton, A. and Chaty, S.: 1999, *IAU Circ.* **7294**
McClintock, J., Remillard, R., Heindl, W., Tomsick, J.: 2000, *IAU Circ.* **7466**

V404 Cyg: 10 years in quiescence *

Elena P. Pavlenko†
Crimean Astrophysical Observatory, Naychny , 98409 Crimea, Ukraine (`pavlenko@crao.crimea.ua`*),*

Yuliana G. Kuznetsova,
Kiev University, Physical Faculty, 64 Volodymyrska Str., Kiev 252017, Ukraine

Sergei Yu. Shugarov and and Vladislav S. Petrov
Sternberg Astronomical Institute, Moscow State University, Universitetskii pr. 13, Moscow, 119899 Russia (`shugarov@sai.msu.ru`*)*

Abstract. We present the preliminary results of a long-term photometric study of V404 Cyg in quiescence. Its ellipsoidal light curves show the variations in both maxima and minima from year to year over 1992-2000. The most prominent are variations of the depth of minimum at phase 0.0 in V (1992-1997) and at phase 0.5 in R (1998-2000). The $\sim 6 - hour$ QPOs persist but with variable amplitude.

Keywords: close binaries, X-ray novae, V404 Cyg

V404 Cyg is one of the brightest objects ($V \sim 18^m$) among known X-ray novae in the quiescent state. It is a black hole X-ray binary (Casares and Charles, 1994), where the mass of the black hole was estimated as $14 - 18M_\odot$ (Antokhina et al., 1993), $\sim 12M_\odot$ (Shahbaz et al., 1994). V404 Cyg has a relatively long orbital period of 6.4714 days and 6-hour QPOs of variable amplitude (up to $0^m.3$) (Pavlenko et al., 1996 and references therein).

Observations of V404 Cyg were carried out during 138 nights: In 1991-1997 at the 0.5-m telescope of the Crimean astrophysical observatory (CrAO) in a broad "B+V" system; in 1998-2000 mostly at 0.38-m Cassegrain telescope (CrAO), also at 1.25-m, 0.6-m and 0.7-m telescopes of the Sternberg Astronomical Institute in a broad "R+I" system (1998-1999) and in R (2000). All data were reduced to the standard V and R system.

The double-humped light curves are believed to be a result of the ellipsoidal effect. We folded our data on the orbital period using the ephemeris (Casares and Charles, 1994) separately in V and R. Phase 0.5 corresponds to the inferior conjunction of the black hole.

For each year we calculated a mean ellipsoidal light curve by least squares fitting the first two harmonics of the orbital period to the data

* The work is partially supported by the RFBR grants RFBI NN 00-15-96553, 00–02–16471, 99–02–16471 and "Astronomy" No 1–4–2–2

† EPP is thankful to Instituto de Astrofisica de Andalucia for supporting her visit to Granada.

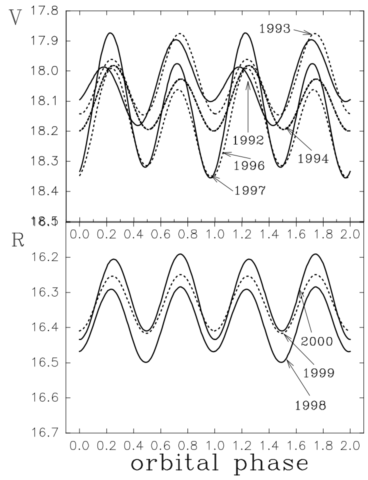

Figure 1. The ellipsoidal light curves evolution in 1992 - 2000.

(Fig. 1). Both minimum and maximum magnitude varies from year to year in both spectral band. In V for 1992-1997 the maximum at phase 0.25 is more stable than that at phase 0.75, and the depth of minimum at phase 0.0 is more variable than that at phase 0.5. In R for 1998-2000 the minimal magnitude variations occur at the minimum at phase 0.0. Since V and R observations were not simultaneous, we cannot conclude whether this behaviour shows dependence on time or on the spectral band. We suggest that changes in accretion disk geometry and brightness with time could produce such lightcurves variations. We also studied the QPO evolution and found that these light oscillations are persistent over all quiescent epochs but display variable amplitude. In 2000 the typical time of the QPOs was 6.26 hours and mean amplitude $0^m.06$.

References

Casares, J. and Charles, P. A. Optical studies of V404 Cyg, the X-ray transient GS2023+338.-IV. The rotation speed of the companion star. *MNRAS*, 271:L5–L9, 1994.

Antokhina, E., Pavlenko, E., Cherepaschuk, A., Shugarov, S. Light curve and parameters of X-ray Nova V404 Cygni - the best black hole candidate". *Astronomy Reports*, 37:407–411, 1993.

Shahbaz, T., Ringwald, F. A., Bunn, J. C. et al. The mass of black hole in V404 Cygni. *MNRAS*, 271:L10–L14, 1994.

Pavlenko, E. P., Martin, A. C., Casares, J. et al. Orbital and quasi-periodic optical variations in the black hole X-ray binary V404 Cyg. *MNRAS*, 281:1094–1104, 1996.